

Evolutionary dynamics of cancer in response to targeted combination therapy

Ivana Bozic^{1,2†}, Johannes G Reiter^{3†}, Benjamin Allen^{1,4†}, Tibor Antal⁵, Krishnendu Chatterjee³, Preya Shah⁶, Yo Sup Moon⁶, Amin Yaqubie⁷, Nicole Kelly⁷, Dung T Le⁸, Evan J Lipson⁸, Paul B Chapman⁷, Luis A Diaz Jr⁹, Bert Vogelstein⁹, Martin A Nowak^{1,2,10*}

¹Program for Evolutionary Dynamics, Harvard University, Cambridge, United States; ²Department of Mathematics, Harvard University, Cambridge, United States; ³Institute of Science and Technology Austria, Klosterneuburg, Austria; ⁴Department of Mathematics, Emmanuel College, Boston, United States; ⁵School of Mathematics, Edinburgh University, Edinburgh, United Kingdom; ⁶Harvard College, Cambridge, United States; ⁷Memorial Sloan-Kettering Cancer Center, New York, United States; ⁸Department of Medical Oncology, Johns Hopkins University School of Medicine; The Sidney Kimmel Comprehensive Cancer Center at Johns Hopkins, Baltimore, United States; ⁹Ludwig Center for Cancer Genetics and Therapeutics, Howard Hughes Medical Institute, Johns Hopkins Kimmel Cancer Center, Baltimore, United States; ¹⁰Department of Organismic and Evolutionary Biology, Harvard University, Cambridge, United States

*For correspondence: martin_nowak@harvard.edu

†These authors contributed equally to this work

Competing interests: The authors declare that no competing interests exist.


Funding: See page 13

Received: 15 March 2013

Accepted: 20 May 2013

Published: 25 June 2013

Reviewing editor: Carl T Bergstrom, University of Washington, United States

 Copyright Bozic et al. This article is distributed under the terms of the [Creative Commons Attribution License](#), which permits unrestricted use and redistribution provided that the original author and source are credited.

Abstract In solid tumors, targeted treatments can lead to dramatic regressions, but responses are often short-lived because resistant cancer cells arise. The major strategy proposed for overcoming resistance is combination therapy. We present a mathematical model describing the evolutionary dynamics of lesions in response to treatment. We first studied 20 melanoma patients receiving vemurafenib. We then applied our model to an independent set of pancreatic, colorectal, and melanoma cancer patients with metastatic disease. We find that dual therapy results in long-term disease control for most patients, if there are no single mutations that cause cross-resistance to both drugs; in patients with large disease burden, triple therapy is needed. We also find that simultaneous therapy with two drugs is much more effective than sequential therapy. Our results provide realistic expectations for the efficacy of new drug combinations and inform the design of trials for new cancer therapeutics.

DOI: [10.7554/eLife.00747.001](https://doi.org/10.7554/eLife.00747.001)

Introduction

The current wave of excitement about targeted cancer therapy (*Sawyers, 2004; Sequist et al., 2008; Kwak et al., 2010; Chapman et al., 2011; Gonzalez-Angulo et al., 2011*) was initiated by the success of imatinib in the treatment of chronic myeloid leukemia (CML) (*Druker et al., 2006; Gambacorti-Passerini et al., 2011*). Four decades of research passed between the discovery of the Philadelphia chromosome and the first treatment to target an activated oncogene in a human cancer. Targeted therapies against many different types of cancer are now being developed at a fast pace. These include gefitinib and erlotinib for non-small-cell lung cancer patients with EGFR mutations (*Sequist et al., 2008*), panitumumab and cetuximab for metastatic colon cancer (*Amado et al., 2008*), vemurafenib for patients with melanomas harboring BRAF mutations (*Chapman et al., 2011*), and crizotinib for lung cancer patients with EML4-ALK translocations (*Kwak et al., 2010*). At present, dozens of other targeted cancer therapies have either been approved or are being evaluated in clinical trials.

eLife digest As medicine becomes increasingly personalized, more and more emphasis is being placed on the development of therapies that target specific cancer-causing mutations. But while many of these drugs are effective in the short term, and do extend patient lives, tumors tend to evolve resistance to them within a few months.

The key problem is that large tumors are genetically diverse. This means that for any given treatment, there is likely to be a small population of cells within the tumor that is resistant to the effects of the drug. When the drug is given to a patient, these cells will survive and multiply and this will lead ultimately to treatment failure. Given that a single drug is therefore highly unlikely to eradicate a tumor, combinations of two or more drugs may offer a higher chance of cure. This approach has been effective in the treatment of HIV as well as certain forms of leukemia.

Here, Bozic et al. present a mathematical model designed to predict the effects of combination targeted therapies on tumors, based on the data obtained from 20 melanoma (skin cancer) patients. Their model revealed that if even 1 of the 6.6 billion base pairs of DNA present in a human diploid cell has undergone a mutation that confers resistance to each of two drugs, treatment with those drugs will not lead to sustained improvement for the majority of patients. This confirms the need to develop drugs that target distinct pathways.

The model also reveals that combination therapy with two drugs given simultaneously is far more effective than sequential therapy where the drugs are used one after the other. Indeed, the model of Bozic et al. indicates that sequential treatment offers no chance of a cure, even when there are no cross-resistance mutations present, whereas combination therapy offers some hope of a cure, even in the presence of cross-resistance mutations.

By emphasizing the need to develop drugs that target distinct pathways, and to administer them in combination rather than sequentially, the study by Bozic et al. offers valuable advice for drug development and the design of clinical trials, as well as for clinical practice.

DOI: [10.7554/eLife.00747.002](https://doi.org/10.7554/eLife.00747.002)

Although targeted agents have prolonged the lives of cancer patients, clinical responses are generally short-lived. In most patients with solid tumors, the cancer evolves to become resistant within a few months (Amado et al., 2008; Sequist et al., 2008; Gerber and Minna, 2010; Chapman et al., 2011). Understanding the evolutionary dynamics of resistance in targeted cancer treatment is crucial for progress in this area and has been the focus of experimental (Engelman et al., 2007; Corcoran et al., 2010; Bivona et al., 2011; Diaz et al., 2012; Ellis et al., 2012; Misale et al., 2012; Straussman et al., 2012; Wilson et al., 2012; Khorashad et al., 2013) and theoretical studies (Dewanji et al., 2005; Komarova and Wodarz, 2005; Michor et al., 2005, 2006; Haeno et al., 2007; Dingli et al., 2008; Katouli and Komarova, 2010; Lenaerts et al., 2010; Beckman et al., 2012; Bozic et al., 2012). One of the most important conclusions of these studies is that a small number of cells resistant to any targeted agent are always present in large solid tumors at the start of therapy and that these cells clonally expand once therapy is administered. Tumor recurrences are thus a fait accompli when single agents are delivered (Diaz et al., 2012).

How can one overcome the near-certainty of disease recurrence following therapy with such agents? Conceptually, there are two paths: treat tumors when they are very small, before a sufficient number of mutant cells conferring resistance have developed, or treat tumors with two or more drugs that target different pathways. In reality, the first option is usually not feasible, as clinicians have little or no control over the size of lesions in their patients at presentation. The second option, however, will become possible as more targeted agents are developed. The potential of combination therapy with targeted agents is buttressed by the success of conventional chemotherapeutic agents in leukemias and other cancers (DeVita, 1975) and of combination therapies for infectious diseases such as HIV (Porter et al., 2003). But the potential therapeutic utility of combination therapies targeting different pathways in solid tumors cannot be inferred from these prior studies, as the anatomic and evolutionary characteristics of solid tumors are far different from those of liquid tumors (leukemias) or infectious diseases. In this work, we have formulated a mathematical model to predict the effects of combined targeted therapies in realistic clinical scenarios and attempted to answer the question posed at the beginning of this paragraph.

Results

Our model is based on a multitype branching process (see ‘Materials and methods’). Similar mathematical modeling has successfully predicted the dynamics of acquired resistance, including the timing of treatment failure, in colorectal cancer patients treated with the EGFR inhibitor panitumumab (Díaz *et al.*, 2012), and has led to specific recommendations for combination therapies to treat CML (Komarova *et al.*, 2009; Katouli and Komarova, 2010). Our current work builds on these previous studies by using recent advances in the mathematical theory of branching processes (Antal and Krapivsky, 2011), which enable us to obtain results that are exact in the biologically relevant limit of many tumor cells and small mutation rate.

To obtain key parameters for our model, we have studied the dynamics of 68 index lesions in 20 melanoma patients receiving the BRAF inhibitor vemurafenib. The data from six patients that represented distinct patterns of responses are shown in **Figure 1**. Patients P1 and P2 achieved complete responses, and their lesions became undetectable. Patient P3 had stable disease, with tumors remaining approximately the same size throughout treatment. Patients P4 to P6 all had partial remissions, with some lesions shrinking and others unchanging or regrowing during treatment. As expected, the smallest lesions were the ones most likely to become undetectable when the agent was effective.

For 21 lesions in our vemurafenib dataset, two pretreatment measurements were available. Using these data, we calculate the average net growth rate of these lesions to be 0.01 per day, which is consistent with previous reports (Friberg and Mattson, 1997; Eskelin *et al.*, 2000). The estimated average time between cell divisions in the absence of cell death in melanoma cells is 7 days (Rew and Wilson, 2000), implying a birth (cell division) rate of $b = 0.14$ per day. We set this as the typical birth rate, and additionally explore birth rates that correspond to a wide range of 1–14 days between cell divisions (**Supplementary file 3**). To achieve the observed net growth rate, we set the cell death rate to $d = b - 0.01$ (typical $d = 0.13$). We assume that these birth and death rates are valid for all cell types prior to treatment. For simplicity, we assume that these birth and death rates remain constant for all cell types prior to treatment, and neglect variations in the growth rate due to spatial and metabolic constraints in solid tumors (Bozic *et al.*, 2012).

A given cancer therapy will reduce the birth rate and/or increase the death rate of tumor cells. A cell type is defined as sensitive if the treatment in question would cause its death rate to exceed its birth rate; otherwise, it is resistant. The key parameters describing a particular combination treatment are its effects on the birth and death rates of cells and the number of point mutations that have the potential to confer resistance. Consider a treatment with two drugs, 1 and 2. We denote by n_1 (respectively, n_2) the number of point mutations that have the potential to confer resistance to drug 1 alone (respectively, drug 2 alone). We denote by n_{12} the number of point mutations that have the potential to confer resistance to both drug 1 and drug 2 (cross-resistance mutations). We assume that drugs in a combination treatment are given at concentrations tolerable by patients, and define the numbers of resistance mutations (n_1 , n_2 , n_{12}) relative to these concentrations (Katouli and Komarova, 2010).

A crucial quantity for the effects of combination therapy is the expected number, X , of resistant cells at the start of treatment in a lesion containing M cells. From the dynamics of our branching process model (see **Supplementary file 1**), we obtain

$$X \approx M \left[n_{12} \mu + \left(n_1 n_2 + \frac{n_{12}}{2} (n_1 + n_2 - n_{12}) \right) \mu^2 \right].$$

Here $\mu = \frac{u}{s} \log(Ms)$ (\log denotes the natural logarithm), where $s = 1 - d/b$ is the survival probability of the branching process initiated with a single cell and u is the point mutation rate, $\sim 10^{-9}$ for most cancers. As μ is small, this formula can be further simplified. If there is at least one possible mutation that could in principle confer resistance to both drugs, $n_{12} \geq 1$, then $X \approx M n_{12} \mu$. In this case, the expected number of cells resistant to both drugs is independent of the numbers of mutations, n_1 and n_2 , that have the potential to confer resistance to each individual drug. Intuitively, this means that tumor cells are much more likely to become resistant to dual therapy through the occurrence of one mutation conferring resistance to both drugs simultaneously than through sequential mutations conferring resistance to each drug separately. If there is no mutation that could confer resistance to both

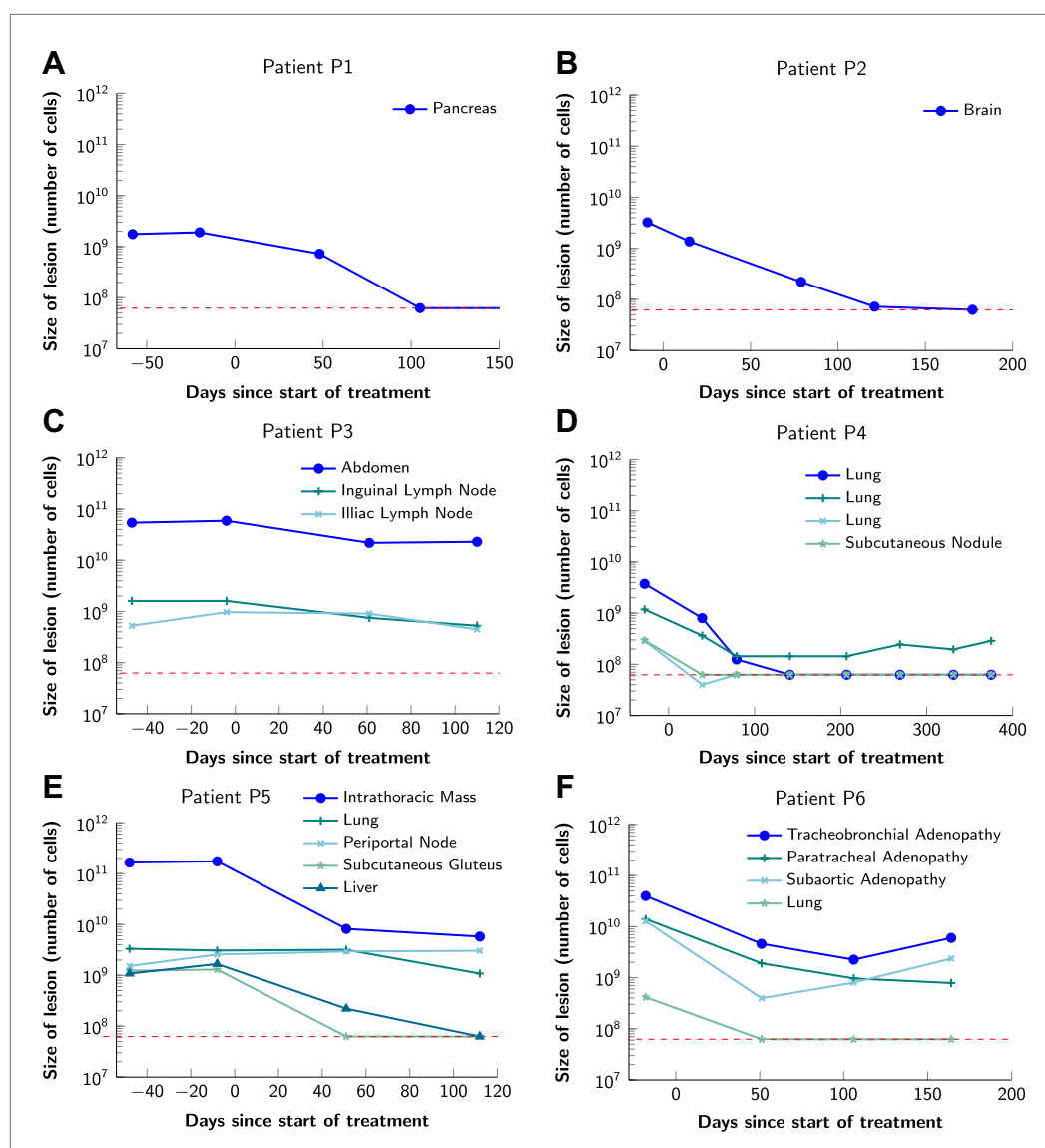


Figure 1. Variability in treatment response to monotherapy among six patients. Patients were treated with the BRAF inhibitor vemurafenib. Patients P1 and P2 achieved a complete response. Patient P3 had stable disease. Patients P4, P5, and P6 had partial responses. The minimal detection size (indicated by discontinuous red line) was assumed to be $\approx 63 \times 10^6$ cells.

DOI: [10.7554/eLife.00747.003](https://doi.org/10.7554/eLife.00747.003)

The following source data are available for figure 1:

Source data 1. Response to vemurafenib.

DOI: [10.7554/eLife.00747.004](https://doi.org/10.7554/eLife.00747.004)

drugs simultaneously (no cross-resistance), then $n_{12} = 0$ and we obtain $X \approx M n_1 n_2 \mu^2$. This quantity scales with the square of the point mutation rate, so the number of resistant cells in a tumor will be much smaller than for the case $n_{12} > 0$. In general, the expected number of cells resistant to combination therapy with k drugs, with no cross-resistance, is $X \approx M n_1 n_2 \dots n_k \mu^k$ (proof in **Supplementary file 1**).

We emphasize, however, that resistance is the outcome of random mutation, division, and death events, and consequently may arise in one lesion but not in another, even if these lesions are otherwise identical. We therefore also obtain formulas for the probability that resistance to combination therapy is present at the time of detection. This probability can be computed as $p_{\text{res}} = 1 - p_1 p_2$. Here, p_1 is the probability that there is no resistance at detection that arose in a single mutational step, due to one of the n_{12} possible cross-resistance mutations. p_2 is the probability that no such resistance arises in two

mutational steps. These probabilities can be expressed as follows (proofs in **Supplementary file 1**, Section 4):

$$p_1 = \exp\left(Mun_{12} \frac{\log(s)}{1-s}\right)$$

$$p_2 \approx \exp\left[Mu^2(2n_1n_2 + n_{12}(n_1 + n_2)) \frac{\log(s)\log(Ms)}{s(1-s)}\right].$$

As above, $s = 1 - d/b$ is the survival probability of the branching process initiated with a single cell. The quantity $2n_1n_2 + n_{12}(n_1 + n_2)$ in the expression for p_2 represents the number of possible two-step mutational paths to dual resistance.

We turn now to the dynamics of the treatment response. Once treatment starts, sensitive cells decline, but resistant cells continue to grow. We assume that resistant cells maintain the pretreatment birth and death rates, b and d , respectively, during treatment. To obtain estimates for the birth rate b' and death rate d' of sensitive cells during treatment, we calculate that the 68 lesions in our dataset declined at median rate $b' - d' = -0.03$ per day (-0.01 and -0.07 being 10th and 90th percentile, respectively). Thus, we set the typical death rate of sensitive cells during treatment to $d' = b' + 0.03$, and additionally explore cases when treatment is less ($d' = b' + 0.01$) or more effective ($d' = b' + 0.07$). As a default in our simulations, we suppose that treatment affects only the death rate ($b' = b$), but our mathematical analysis applies also to the case that treatment affects the birth rate.

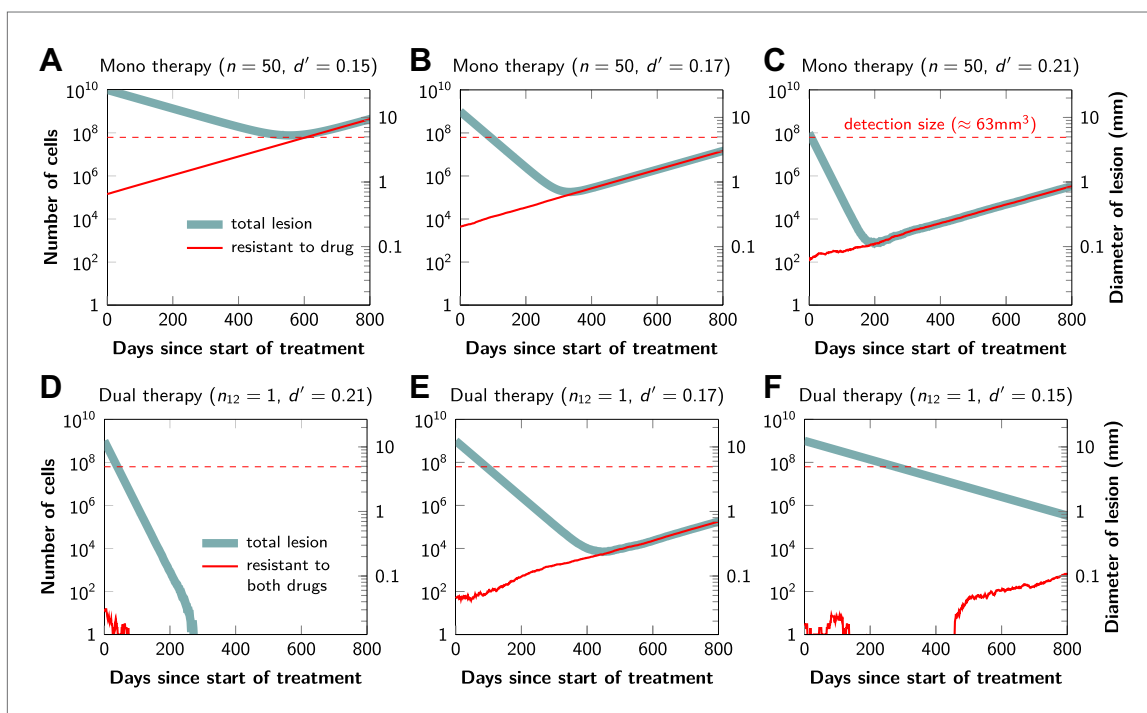


Figure 2. Tumor response to mono and dual therapy. The tumor grows exponentially until a certain detection size, M , is reached, at which point treatment is initiated. The number of point mutations that could in principle confer resistance to monotherapy is $n = 50$. For dual therapy, the number of point mutations that could confer resistance to drugs 1 and 2 separately is given by $n_1 = 50$ and $n_2 = 50$. The number of point mutations that could confer resistance to both drugs simultaneously is given by n_{12} . The point mutation rate was assumed to be $u = 10^{-9}$ and the rate of cell division $b = 0.14$ per day and is unaffected by treatment. The rate of cell death before treatment is $d = 0.13$ per day; it is increased to d' for sensitive cells during treatment. (A)–(C) For clinically detectable sizes ($M = 10^{10}, 10^9, 10^8$, depending on the location of the tumors and the detection methods used), monotherapy leads to a temporary shrinkage of the tumor but is always followed by tumor regrowth. (D) Due to stochastic fluctuations the few resistant cells present at the start of treatment go extinct and the lesion is eradicated. (E) Treatment leads to a temporary shrinkage of the tumor followed by regrowth. (F) The tumor decreases slowly in response to dual therapy, but resistant cells eventually evolve and cause treatment failure.

DOI: [10.7554/eLife.00747.005](https://doi.org/10.7554/eLife.00747.005)

Figure 2 shows computer simulations of single lesions in response to targeted therapies. Previous studies (Engelman et al., 2007; Corcoran et al., 2010; Diaz et al., 2012; Ellis et al., 2012; Misale et al., 2012; Straussman et al., 2012; Wilson et al., 2012) suggest that about 50 different mutations can confer resistance to a typical targeted therapeutic agent. Assuming that there are 50 or more potential resistance mutations, monotherapy will eventually fail in all lesions that can be detected by conventional imaging (**Figure 2A,B**) even when the death rate d' conferred by the therapy is far higher than usually observed in practice (**Figure 2C**). Small lesions, however, can decrease below the detection limit and appear to be eradicated for years before re-emerging (**Figure 2B,C**). This result is important, as it explains why tumors can recur after long periods of remission without the need to invoke processes involving cancer stem cells, angiogenesis, or immune escape (Hensel et al., 2012). Note that results similar to those obtained by simulation are observed in several of the individual lesions from actual patients graphed in **Figure 1**.

The results predicted to occur with dual therapy are shown in **Figure 2D–F**. Here, we also assume that there are 50 mutations that have the potential to confer resistance to either drug alone, but also that there is at least one mutation that can confer resistance to both drugs simultaneously. Intuitively, one might imagine that the existence of even a single cell resistant to both drugs at the start of therapy will automatically result in treatment failure. However, our results show that this is not necessarily true, and that the response depends on the size of the lesion, the number of cross-resistant cells, and the effects of the therapy on the balance between cell birth and cell death. Three examples illustrate these points. In **Figure 2D**, there is a small number of cells resistant to both drugs at the initiation of dual therapy, but these cells are lost by stochastic drift and the lesion is eradicated. In **Figure 2E**, there is a greater, but still relatively small number (~100), of cells resistant to both drugs. The lesion shrinks at first, but eventually progresses due to preexisting cross-resistance mutations within it. In the third lesion, the few cells resistant to both drugs at the initiation of therapy are lost to stochastic drift, but the cytolytic effects of the drug combination are less pronounced than in the other two cases ($d' = 0.15$ instead of 0.17 or 0.21). The relatively slow decrease in lesion size enables the generation of de novo resistance mutations during treatment and the lesion eventually recurred (**Figure 2F**).

In summary, treatment failure can be caused either by the preexistence of resistance to both drugs in a small number of tumor cells (**Figure 2E**) or the emergence of resistant cells during treatment (**Figure 2F**). Taking both of these possibilities into account, the probability, p_{erad} , that dual therapy eradicates a lesion containing M cells at the start of treatment is given by

$$p_{\text{erad}} = p_1^{\uparrow} p_1^{\downarrow} p_2^{\uparrow} p_2^{\downarrow}. \quad (1)$$

p_1^{\uparrow} is the probability that no 1-step resistant lineage arises (and survives) prior to treatment. p_1^{\downarrow} is the probability that no 1-step resistant lineage arises (and survives) during treatment. p_2^{\uparrow} is the probability that no 2-step resistant lineage arises (and survives) prior to treatment. p_2^{\downarrow} is the probability that no 2-step resistant lineage arises (and survives) during treatment. Here, 'steps' refers to the number of mutations (one or two) needed to achieve dual resistance, and 'lineage' refers to the descendants of a single cell that has achieved dual resistance via a particular mutational path. The therapy is successful if there is no resistant lineage arising in any of these four scenarios; since these are independent events, the overall success probability is obtained by multiplying the corresponding probabilities as shown in **equation (1)**. The probabilities that no 1-step resistant lineages arise before (p_1^{\uparrow}) or during treatment (p_1^{\downarrow}) and survive are given by Komarova and Wodarz (2005)

$$p_1^{\uparrow} = \exp(-Mun_{12})$$

and Michor et al. (2006)

$$p_1^{\downarrow} = \exp\left(Mun_{12} \frac{s}{s'}\right).$$

Here $s = 1 - d/b$ as above, and $s' = 1 - d'/b'$, where b' and d' are birth and death rates of cells sensitive to at least one drug during treatment (note that $s' < 0$). The probabilities that no 2-step resistant lineages arise before (p_2^\uparrow) or during (p_2^\downarrow) treatment and survive can be calculated as:

$$p_2^\uparrow = \exp \left[Mu^2 \frac{s' - s}{ss'} \left(n_1(n_2 + n_{12}) \log \left(\frac{1}{sM} + u(n_2 + n_{12}) \frac{s' - s}{ss'} \right) + n_2(n_1 + n_{12}) \log \left(\frac{1}{sM} + u(n_1 + n_{12}) \frac{s' - s}{ss'} \right) \right) \right]$$

and

$$p_2^\downarrow = \exp \left(-Mu^2 (2n_1n_2 + n_{12}(n_1 + n_2)) \frac{s}{s'^2} \right).$$

The proofs of these results are provided in **Supplementary file 1**, Section 5. Excellent agreement between **equation (1)** and simulation results is shown in **Figure 3**.

Although modeling of single neoplastic lesions is the norm in theoretical studies, most patients with advanced cancers have multiple lesions and curing a patient requires eradication of all lesions. **Equation (1)** can be used to evaluate which combination treatments will be successful in typical patients with multiple metastatic lesions.

To determine the total extent of disease in typical patients who enroll for clinical trials, we quantified all radiographically detectable metastases in 22 such patients: 7 with pancreatic ductal adenocarcinomas, 11 with colorectal carcinomas, and 6 with melanomas—a different cohort than that depicted in **Figure 1**, in which only index lesions (those easiest to measure) were evaluated. The number of metastatic lesions in the 22 patients described in **Table 1** ranged from 1 to 30, and their total tumor burden ranged from 9×10^8 to 3×10^{11} cells (see **Supplementary file 2**).

For each of these 22 patients, we used **equation (1)** to calculate the probability that monotherapy or dual therapy would eradicate all the patients' lesions. We find that monotherapy will fail in all 22 patients (**Table 1** and **Supplementary file 3**), as expected from the simulations in **Figure 2A–C** and

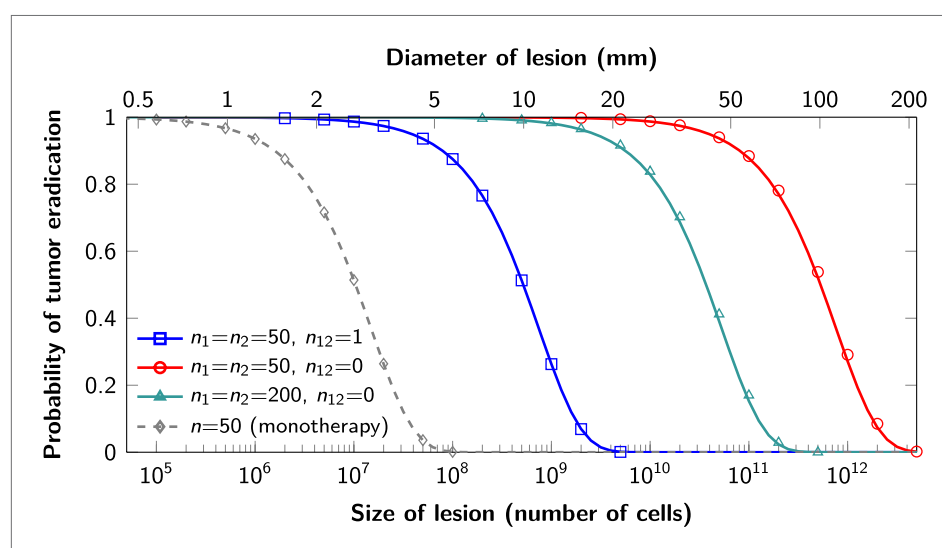


Figure 3. Probability of tumor eradication for two-drug combination therapy. A single mutation conferring cross-resistance to both drugs ($n_{12} = 1$) can prohibit any hope for a successful dual therapy. Solid curves show analytical results for dual therapy and dashed curve shows analytical results for a typical monotherapy, both are calculated using **equation (1)**. Markers (square, triangle, circle, diamond) indicate simulation results (averages of 10^6 runs). Parameter values: birth rate $b = 0.14$, death rate $d = 0.13$, death rate for sensitive cells during treatment $d' = 0.17$, point mutation rate $u = 10^{-9}$. DOI: [10.7554/eLife.00747.006](https://doi.org/10.7554/eLife.00747.006)

Table 1. Probability of treatment failure for combination therapy in patients

Patient	Primary tumor type	Number of metastases	Total tumor burden (number of cells)	Probability of treatment failure		
				Monotherapy	Dual therapy: $n_{12} = 1$	Dual therapy: $n_{12} = 0$
N1	Pancreas	18	2.6×10^{11}	1	1	0.283
N2	Colon	25	2.3×10^{11}	1	1	0.26
N3	Melanoma	26	1.7×10^{11}	1	1	0.203
N4	Melanoma	30	1.4×10^{11}	1	1	0.172
N5	Colon	21	1.0×10^{11}	1	1	0.128
N6	Melanoma	8	9.8×10^{10}	1	1	0.12
N7	Colon	25	9.1×10^{10}	1	1	0.112
N8	Pancreas	8	7.4×10^{10}	1	1	0.092
N9	Pancreas	23	6.4×10^{10}	1	1	0.08
N10	Pancreas	5	5.5×10^{10}	1	1	0.069
N11	Colon	14	5.4×10^{10}	1	1	0.068
N12	Rectal	23	4.8×10^{10}	1	1	0.061
N13	Melanoma	9	4.1×10^{10}	1	1	0.052
N14	Pancreas	13	4.1×10^{10}	1	1	0.051
N15	Pancreas	8	3.3×10^{10}	1	1	0.042
N16	Melanoma	7	2.2×10^{10}	1	1	0.028
N17	Melanoma	10	2.1×10^{10}	1	1	0.027
N18	Colon	4	2.0×10^{10}	1	1	0.026
N19	Melanoma	9	1.8×10^{10}	1	1	0.023
N20	Colon	3	1.6×10^9	1	0.881	0.002
N21	Melanoma	21	1.3×10^9	1	0.828	0.002
N22	Pancreas	1	8.5×10^8	1	0.677	0.001

For monotherapy, we assume that 50 point mutations ($n = 50$) can in principle confer resistance to the drug. With dual therapy, we assume that 50 point mutations can in principle confer resistance to each drug individually ($n_1 = n_2 = 50$). Two scenarios are modeled: in the first, there is one mutation that can in principle confer resistance to both drugs (i.e., cross-resistance, $n_{12} = 1$). In the other case, there are no possible mutations that can confer resistance to both drugs ($n_{12} = 0$). Parameter values: birth rate, $b = 0.14$, death rate, $d = 0.13$, death rate for sensitive cells during treatment, $d' = 0.17$, point mutation rate $u = 10^{-9}$. Colon: colonic adenocarcinoma; Rectal: rectal adenocarcinoma; Pancreas: pancreatic ductal adenocarcinoma. DOI: [10.7554/eLife.00747.007](https://doi.org/10.7554/eLife.00747.007)

from clinical experience. If there is even one possible mutation that can in principle confer resistance to both drugs, then our model shows that dual therapy has also only a small chance of curing patients, even those with the smallest tumor burden. In our cohort of 22 patients, none are expected to be cured under these circumstances (Table 1). Only if there are no potential mutations that can confer cross-resistance will dual therapy be successful in eradicating all lesions. In the cohort described in Table 1, we calculate that eight patients (those with the smallest tumor burden) would have >95% probability of cure. Those with the largest tumor burden would still have a >20% probability of tumor recurrence. Additional simulations show that therapy with three agents will also not cure patients if there is even one mutation that can confer resistance to all three agents. Similar conclusions hold if we vary parameter values within a reasonable range (Supplementary file 3). We note that in patients whose tumors have high cell turnover (time between cell divisions of 1 day, corresponding to $b = 1$), even dual therapy with no cross-resistance mutations would be expected to fail in 37% of patients described in Table 1 (Supplementary file 3).

Graphical representations of the simulated responses of two patients with multiple metastatic lesions are shown in Figure 4. With monotherapy in patient N1 (Figure 4A), all lesions are predicted

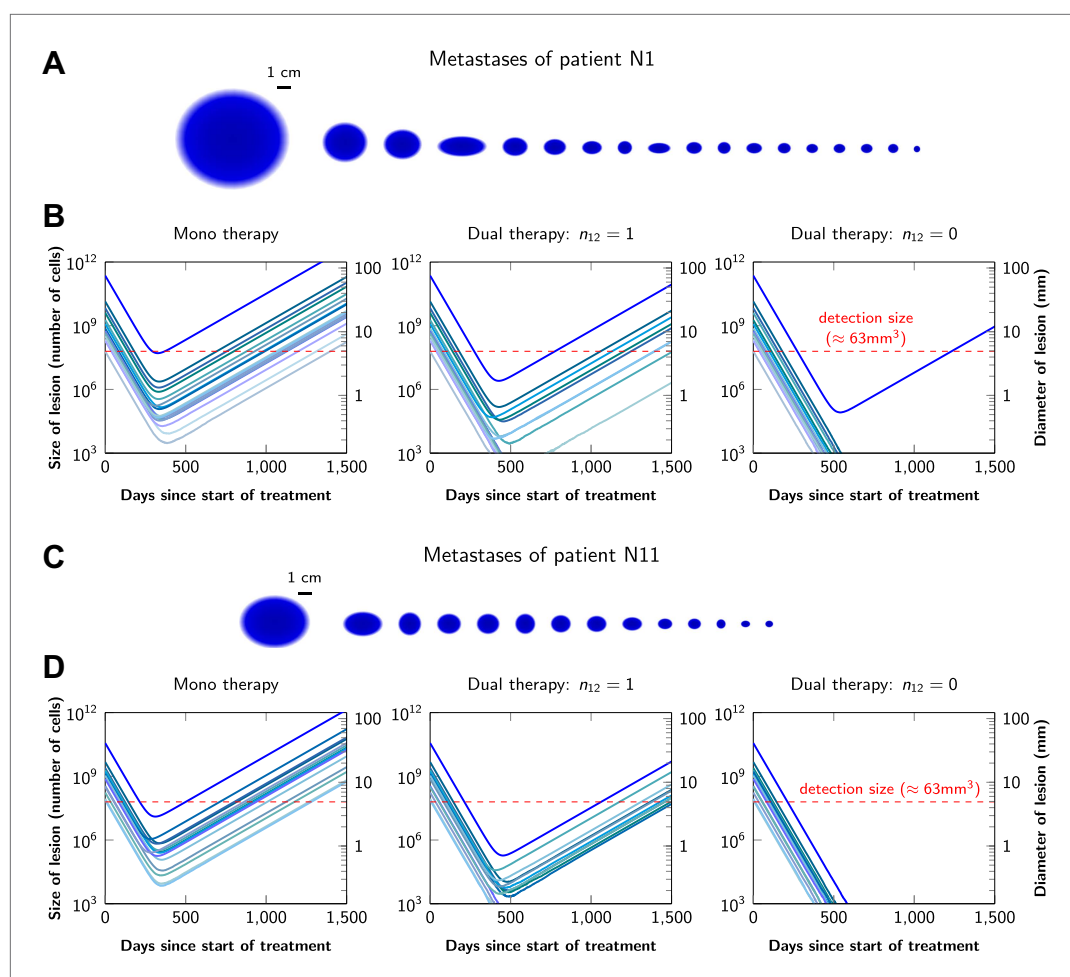


Figure 4. Treatment response dynamics to monotherapy and dual therapy in two patients. (A) Depiction of all 18 detectable metastases in patient N1, who had a particularly heavy tumor burden (scale 1:4). (B) Simulated treatment of patient N1, comparing monotherapy with $n = 50$ resistance mutations to the individual drugs and dual therapy with $n_1 = n_2 = 50$ resistance mutations to the individual drugs and one ($n_{12} = 1$) or no ($n_{12} = 0$) cross-resistance mutations to both drugs. (C) Depiction of all 14 detectable metastases in patient N11, who had a more typical tumor burden (scale 1:4). (D) Simulated treatment of patient N11. Parameter values for simulations in (B) and (D): birth rate $b = 0.14$; death rate $d = 0.13$; death rate for sensitive cells during treatment $d' = 0.17$; point mutation rate $u = 10^{-9}$. DOI: 10.7554/eLife.00747.008

to regress, but then recur within a year or so after the initiation of therapy (Figure 4B, left panel). Treatment failure in most lesions would also occur after dual therapy when there is at least one mutation that could confer resistance to both agents, although the length of remission will be longer than with monotherapy (Figure 4B, middle panel). In patient N11, with less disease burden, dual therapy will fail to eradicate several of the lesions when there is a possibility of a single cross-resistance mutation, but there is hope of cure if no such cross-resistance mutations are possible (Figure 4C,D).

In current clinical practice, it is common to administer targeted agents sequentially: once relapse occurs, a second, often experimental, agent is administered. The model described above can also be used to predict the relative effectiveness of sequential vs simultaneous therapies of a single lesion with two drugs. When there is a possibility of a single mutation conferring resistance to both drugs, sequential combination therapy will 'always' fail. In ~74% of lesions, the failure is due to mutations that were present prior to the treatment with the first drug, whereas in ~26% of the lesions, failure is due to the development of cells resistant to drug 2 during treatment with drug 1 (Figure 5A and Figure 5—figure supplement 1). With simultaneous treatment, it is possible to eradicate ~26% of the lesions even when cross-resistance mutations are possible (Figure 5B). When there is no possibility of a mutation conferring cross-resistance to

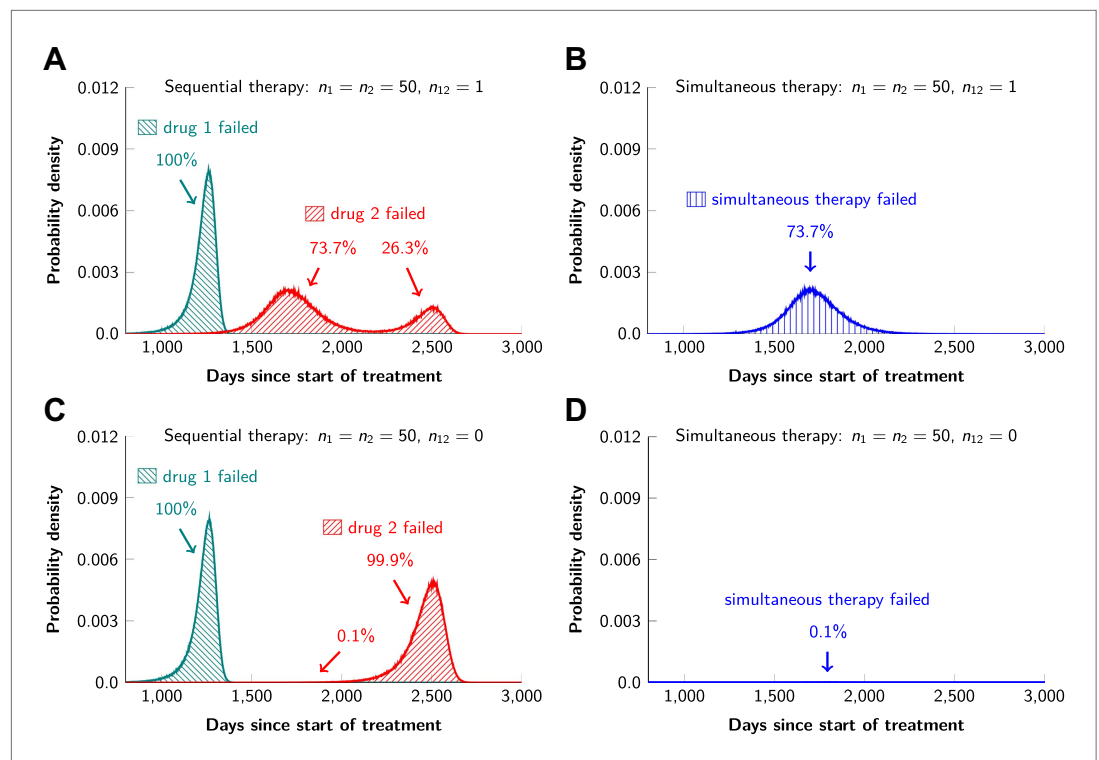


Figure 5. Sequential vs simultaneous therapy with two drugs. (A) If there is even a single mutation that confers cross-resistance to both drugs ($n_{12} = 1$), then sequential therapy will fail in all cases. In 73.7% of the cases, this failure is due to the exponential growth of fully resistant cells that were present at the start of treatment. In the remaining 26.3% of cases, the failure is due to resistance mutations that developed during therapy with the first drug. (B) With simultaneous therapy, 26.3% of patients can be cured under the same circumstances. In the remaining patients (73.7%), cross-resistant mutations existed prior to the therapy and their expansive growth will ensure treatment failure whether treatment is simultaneous or sequential (see **Figure 5—figure supplement 1** for further details). (C) and (D) If the two drugs have no resistance mutations in common ($n_{12} = 0$), then simultaneous therapy is successful with a probability of 99.9% while sequential therapy still fails in all cases.

DOI: [10.7554/eLife.00747.009](https://doi.org/10.7554/eLife.00747.009)

The following figure supplements are available for figure 5:

Figure supplement 1. Examples for the evolution of resistance during sequential therapy.

DOI: [10.7554/eLife.00747.010](https://doi.org/10.7554/eLife.00747.010)

both drugs, the differences are even more striking: sequential therapy fails in 100% of cases (**Figure 5C**), whereas simultaneous therapy succeeds in >99% of lesions of the identical size (**Figure 5D**).

One of the most important aspects of the cancer stem cell hypothesis revolves around therapeutic resistance. Evidence to date does not indicate that cancer stem cells are innately resistant to either single drugs or drug combinations. However, the precise proportion of cancer stem cells (among all cancer cells) has a dramatic effect on the development of resistance. This effect can be studied using our model if we use the number of cancer stem cells as an effective population size in our formulas and adjust other parameters to account for the stem cell dynamics (**Tomasetti and Levy, 2010**) (i.e., the birth rate should correspond to the rate of symmetric renewal, the rate of symmetric differentiation should be added to the death rate, and an effective mutation rate for stem cells should be introduced to account for mutations that occur during asymmetric division). For example, if cancer stem cells represent only 0.1% of cancer cells, then the development of resistance to single agents or combinations is roughly 0.1% as likely as if 100% of the cancer cells have the capacity to repopulate the tumor. The fraction of cancer stem cells appears to be this low in CML, perhaps explaining the remarkable success of imatinib (**Michor et al., 2005**). In solid tumors, however, the fraction of cancer stem cells seems much higher, usually higher than 5% and in some cases close to 100% (**Shackleton et al., 2009**). This issue is further complicated by the fact that the situation is plastic, with non-stem cells converting to cancer stem cells under certain conditions (**Gupta et al., 2009**). As better approaches to quantify

cancer stem cells in solid tumors become available, our estimates of the likelihood of therapeutic success will be improved.

If resistance has a fitness cost, then we expect a smaller number of resistant cells at the start of treatment and correspondingly a higher chance of treatment success. We used computer simulations to verify our results in the case when there is a cost for resistance, by assuming that each resistance mutation decreases the net growth rate of the cell by up to 10%. The results are shown in **Table 2**. For combination therapies with drugs that have resistance mutations in common, the probability of eradicating a lesion is only marginally affected by costly resistance. For dual therapies with no cross-resistance mutations, treatment has a high chance of eradicating all but the largest lesions, whether or not resistance is costly. In the case of large lesions with high cell turnover rates (the case in which even dual therapies with no cross-resistance might fail), costly resistance increases the chance of treatment success. For example, if each resistance mutation decreases the net growth rate of cells by 10%, the probability that dual therapy with no cross-resistance mutations will eradicate a lesion of size 10^{11} in which cells divide on average every day is 68% (compared with 47% in the case of neutral resistance).

Some therapies may directly eliminate tumor cells ($d' > d$), whereas others may impede their division ($b' < b$). Our formulas account for both of these possibilities. Overall, the rate $b' - d'$ of tumor decline is of primary importance, and whether this is achieved by eliminating cells or suppressing division has only a minor effect on treatment outcomes. For example, consider a dual therapy with $n_1 = n_2 = 50$, $n_{12} = 1$, applied to a lesion of size $M = 10^9$, with other parameters as inferred from our dataset. If this therapy shrinks the tumor at rate -0.03 per day by increasing cell death, the eradication probability is 26%. If the therapy instead suppresses division, this probability increases to 29%, because there are fewer chances for resistance mutations during treatment.

While our typical parameter values are derived from the melanoma dataset, our analytical results can accommodate parameter values from any other type of cancer, once they become available. Furthermore, our results are qualitatively robust across a wide range of birth and death rates (**Supplementary file 3**). The parameters with the strongest effects on the success of combination treatments—apart from the number of cross-resistance mutations—are lesion sizes and point mutation rate. Thus, we expect that combination treatments will be more effective in cancers with small fractions of tumor stem cells (small effective population size of lesions) and less effective in cancers with significantly increased point mutation rates.

Discussion

Our conclusions are highly relevant for the expanding development and use of targeted agents for cancer therapy. Most importantly, they show that even if there is one genetic alteration within any of the 6.6 billion base pairs present in a human diploid cell that can confer resistance to two targeted agents, therapy with those agents will not result in sustained benefit for the majority of patients with advanced disease. The same result is obtained with triple therapy; if there is the possibility of a mutation

Table 2. Simulation results for the probability of treatment failure when resistance is costly

Dual therapy:		Number of cells	Birth rate	Probability of treatment failure			
$n_1 = n_2$	n_{12}			$c = 0\%$	$c = 1\%$	$c = 5\%$	$c = 10\%$
50	0	10^9	0.14	0.0	0.0	0.0	0.0
50	0	10^9	1	0.01	0.01	0.01	0.0
50	1	10^9	0.14	0.74	0.73	0.72	0.7
50	1	10^9	1	0.74	0.74	0.72	0.7
50	0	10^{11}	0.14	0.12	0.11	0.08	0.06
50	0	10^{11}	1	0.53	0.51	0.42	0.32
50	1	10^{11}	0.14	1.0	1.0	1.0	1.0
50	1	10^{11}	1	1.0	1.0	1.0	1.0

Each resistance mutation reduces the net growth rate by a factor c via a decrease of the birth rate b . Parameter values are death rate, $d = b - 0.01$, death rate for sensitive cells during treatment, $d' = b + 0.03$, point mutation rate, $u = 10^{-9}$. The simulation results are averages over 10^4 runs per parameter combination.
[DOI: 10.7554/eLife.00747.011](https://doi.org/10.7554/eLife.00747.011)

conferring cross-resistance to three drugs, lesions of the size commonly observed in patients with advanced cancers will always recur. Similar conclusions were reached by [Komarova et al. \(2009\)](#), who showed that a combination of three current targeted drugs for CML will not be beneficial over a combination of two such drugs due to cross-resistance. Our formulas could be used to develop an optimum in vitro assay to detect the existence of cross-resistance mutations for a given drug combination.

The development of drugs that act through distinct pathways will therefore be essential for the success of combination therapies in the clinic. Although this seems feasible in principle, there are a number of observations suggesting that it will be difficult in practice. For example, it has been shown that the increased expression of growth factors (such as hepatocyte growth factor) can confer resistance to a variety of drugs that inhibit kinases functioning through different pathways ([Straussman et al., 2012](#); [Wilson et al., 2012](#)). Moreover, it is well known that mutations in several different genes, including those encoding ABC transporters, can confer resistance to many different drugs ([Lavi et al., 2012](#)). Drugs that have very different chemical structures, in addition to distinct mechanisms of action, may be required to circumvent these resistance mechanisms.

Our results are not readily applicable to therapies that rely on the immune destruction of tumors ([Kirkwood et al., 2012](#)), such as those employing CTLA-4 ([Hodi et al., 2010](#)), PD1 ([Topalian et al., 2012](#)), or CD19-CARs ([Grupp et al., 2013](#)). This promising line of therapy relies on an ongoing battle between cancer cells and the immune system. The immune system, unlike small molecule compounds, can replicate and evolve, and the factors underlying therapeutic success or failure are not sufficiently understood to allow useful modeling at this point. Once the mechanisms underlying the failures of immune modulators become more apparent, it will be important to try to understand why long-term control of disease is more common with these therapies than with small molecule drugs.

Our results on sequential vs simultaneous therapy with two or more agents ([Figure 5](#)) are in agreement with previous results ([Katouli and Komarova, 2011](#)) and have immediate practical implications even while new combinations are being developed. Sequential administration of targeted agents is often used to treat patients, for a variety of medical and economic reasons. Our data show that this sequential administration precludes any chance for cure—even when there are no possible mutations that can confer cross-resistance ([Figure 5C](#)). And when there are potential mutations conferring cross-resistance to two or more agents, simultaneous administration offers some hope for cure while there is no hope with sequential therapy ([Figure 5A](#)). The realization of the advantages of simultaneous vs sequential dual therapy will hopefully stimulate efforts to combine agents much earlier in the drug development process.

Materials and methods

Model

We model tumor growth and evolution as a continuous time multitype branching process ([Athreya and Ney, 1972](#); [Goldie and Goldman, 1998](#); [Komarova and Wodarz, 2005](#)). In the case of two drugs, there are four possible types: 00, 01, 10, and 11, where zeros indicate sensitivity to a drug and ones indicate resistance. For example, type 01 is sensitive to drug 1 and resistant to drug 2.

Our model includes two phases: pretreatment and treatment. The pretreatment phase is initiated with a single fully sensitive cell (type 00 for two drugs). During this phase, all cell types reproduce at rate b and die at rate d . The offspring of a type 00 cell has probability u_1 of being type 10, u_2 of being type 01, u_{12} of being type 11, and otherwise is of type 00. The offspring of a type 10 cell has probability u ($n_2 + n_{12}$) of being of type 11 and otherwise is of type 10; similar probabilities apply to type 01. Type 11 cells produce only type 11. These formulas generalize in straightforward manner to combination therapy with three or more drugs.

The pretreatment phase ends, and the treatment phase begins, when there are a total of M cells. During the treatment phase, all cell types that are sensitive to one or more drugs have birth rate b' and death rate d' ; fully resistant cells maintain the pretreatment birth and death rates. Mutation probabilities are unchanged.

Analysis

Our mathematical analysis of dual therapy is based in part on a recently discovered exact solution to the two-type branching process ([Antal and Krapivsky, 2011](#)). Detailed proofs of all results are provided in [Supplementary file 1](#).

Computer simulations

We use Monte Carlo computer simulations to confirm our analytical results and improve our understanding of the evolutionary dynamics during cancer treatment. The developed tool is an enhanced version of TTP (Tool for Tumor Progression) where the discrete time branching processes are replaced by continuous time branching processes (Reiter et al., 2013). Moreover, the new version also simulates tumor dynamics during treatment with several drugs. The simulations implement a multitype birth–death branching process using the specified parameter values. For cell subpopulations with less than 10⁴ cells, the process is simulated exactly; for larger subpopulations, a deterministic (exponential growth) approximation is used in the interest of efficiency. Within this deterministic approximation, the timing of appearances of new mutations is simulated using an adapted version of the Gillespie algorithm (Gillespie, 1977). Between 10⁶ and 10⁸ runs are used for each parameter combination.

To study the consequences of costly resistance, we suppose that each resistance mutation reduces the cell division rate such that the net growth rate is decreased by a factor *c* representing the metabolic costs of resistance. For example, cells with two resistance mutations divide at rate $(b - d)(1 - c)^2 + d$.

Additional information

Funding

Funder	Grant reference number	Author
Foundational Questions in Evolutionary Biology Fund		Ivana Bozic, Benjamin Allen, Tibor Antal, Martin A Nowak
European Research Council Start Grant	279307	Johannes G Reiter, Krishnendu Chatterjee
FWF (The Austrian Science Fund) Grant	S11407-N23, P23499-N23	Johannes G Reiter, Krishnendu Chatterjee
Microsoft Faculty Fellow Award		Johannes G Reiter, Krishnendu Chatterjee
The John Templeton Foundation		Martin A Nowak
The Danny Federici Melanoma Fund		Paul B Chapman
John Figge Melanoma Fund		Paul B Chapman
The Virginia and D. K. Ludwig Fund for Cancer Research		Luis A Diaz Jr, Bert Vogelstein
National Cancer Institute	contract N01-CN-43309	Luis A Diaz Jr, Bert Vogelstein
National Institutes of Health	CA129825, CA43460, CA57345	Luis A Diaz Jr, Bert Vogelstein
National Colorectal Cancer Research Alliance		Luis A Diaz Jr, Bert Vogelstein

The funders had no role in study design, data collection and interpretation, or the decision to submit the work for publication.

Author contributions

IB, JGR, BA, MAN, Designed the study, performed mathematical analysis and computer simulations, analyzed data and wrote the manuscript; TA, KC, Performed mathematical analysis and computer simulations, provided input to the manuscript; PS, YSM, AY, NK, DTL, EJJ, PBC, LAD, Contributed data, analyzed data and provided input to the manuscript; BV, Designed the study, contributed data, analyzed data and wrote the manuscript

Ethics

Human subjects: Work was reviewed by the institutional review board of Memorial-Sloan Kettering Cancer Center and was granted an exemption as per 45 CFR 46.101.b (4). A waiver for HIPAA Authorization and informed consent was granted as per 45 CFR 164.512(i)(2)(ii) and 45 CFR 46.116(d). The study protocols (ClinicalTrials.gov # NCT01459614 and Johns Hopkins Protocol # J0545 and J0746) were approved by the Johns Hopkins Institutional Review Boards and all patients signed a written consent form.

Additional files

Supplementary files

- Supplementary file 1. Mathematical proofs.
DOI: [10.7554/eLife.00747.012](https://doi.org/10.7554/eLife.00747.012)
- Supplementary file 2. Lesion sizes of patients who failed conventional treatments.
DOI: [10.7554/eLife.00747.013](https://doi.org/10.7554/eLife.00747.013)
- Supplementary file 3. Probability of combination therapy failure in patients.
DOI: [10.7554/eLife.00747.014](https://doi.org/10.7554/eLife.00747.014)

References

- Amado RG, et al. 2008. Wild-type KRAS is required for panitumumab efficacy in patients with metastatic colorectal cancer. *J Clin Oncol* **26**:1626–34. doi: [10.1200/JCO.2007.14.7116](https://doi.org/10.1200/JCO.2007.14.7116).
- Antal T, Krapivsky PL. 2011. Exact solution of a two-type branching process: models of tumor progression. *J Stat Mech* doi: [10.1088/1742-5468/2011/08/P08018](https://doi.org/10.1088/1742-5468/2011/08/P08018).
- Athreya KB, Ney PE. 1972. *Branching Processes*. Berlin: Springer-Verlag.
- Beckman RA, Schemmann GS, Yeang CH. 2012. Impact of genetic dynamics and single-cell heterogeneity on development of nonstandard personalized medicine strategies for cancer. *Proc Natl Acad Sci USA* **109**:14586–91. doi: [10.1073/pnas.1203559109](https://doi.org/10.1073/pnas.1203559109).
- Bivona TG, et al. 2011. FAS and NF-kappaB signalling modulate dependence of lung cancers on mutant EGFR. *Nature* **471**:523–6. doi: [10.1038/nature09870](https://doi.org/10.1038/nature09870).
- Bozic I, Allen B, Nowak MA. 2012. Dynamics of targeted cancer therapy. *Trends Mol Med* **18**:311–6. doi: [10.1016/j.molmed.2012.04.006](https://doi.org/10.1016/j.molmed.2012.04.006).
- Chapman PB, et al. 2011. Improved survival with vemurafenib in melanoma with BRAF V600E mutation. *N Engl J Med* **364**:2507–16. doi: [10.1056/NEJMoa1103782](https://doi.org/10.1056/NEJMoa1103782).
- Corcoran RB, et al. 2010. BRAF gene amplification can promote acquired resistance to MEK inhibitors in cancer cells harboring the BRAF V600E mutation. *Sci Signal* **3**:ra84. doi: [10.1126/scisignal.2001148](https://doi.org/10.1126/scisignal.2001148).
- DeVita VT Jnr. 1975. Single agent versus combination chemotherapy. *CA Cancer J Clin* **25**:152–8. doi: [10.3322/canjclin.25.3.152](https://doi.org/10.3322/canjclin.25.3.152).
- Dewanji A, Luebeck EG, Moolgavkar SH. 2005. A generalized Luria-Delbruck model. *Math Biosci* **197**:140–52. doi: [10.1016/j.mbs.2005.07.003](https://doi.org/10.1016/j.mbs.2005.07.003).
- Diaz LA Jnr, et al. 2012. The molecular evolution of acquired resistance to targeted EGFR blockade in colorectal cancers. *Nature* **486**:537–40. doi: [10.1038/nature11219](https://doi.org/10.1038/nature11219).
- Dingli D, Traulsen A, Pacheco JM. 2008. Chronic myeloid leukemia: origin, development, response to therapy, and relapse. *Clin Leuk* **2**:133–9. doi: [10.3816/CLK.2008.n.017](https://doi.org/10.3816/CLK.2008.n.017).
- Druker BJ, et al. 2006. Five-year follow-up of patients receiving imatinib for chronic myeloid leukemia. *N Engl J Med* **355**:2408–17. doi: [10.1056/NEJMoa062867](https://doi.org/10.1056/NEJMoa062867).
- Ellis MJ, et al. 2012. Whole-genome analysis informs breast cancer response to aromatase inhibition. *Nature* **486**:353–60. doi: [10.1038/nature11143](https://doi.org/10.1038/nature11143).
- Engelman JA, et al. 2007. MET amplification leads to gefitinib resistance in lung cancer by activating ERBB3 signaling. *Science* **316**:1039–43. doi: [10.1126/science.1141478](https://doi.org/10.1126/science.1141478).
- Eskelin S, Pyrhonen S, Summanen P, Hahka-Kemppinen M, Kivela T. 2000. Tumor doubling times in metastatic malignant melanoma of the uvea: tumor progression before and after treatment. *Ophthalmology* **107**:1443–9. doi: [10.1016/S0161-6420\(00\)00182-2](https://doi.org/10.1016/S0161-6420(00)00182-2).
- Friberg S, Mattson S. 1997. On the growth rates of human malignant tumors: implications for medical decision making. *J Surg Oncol* **65**:284–97. doi: [10.1002/\(SICI\)1096-9098\(199708\)65:43.O.CO;2-2](https://doi.org/10.1002/(SICI)1096-9098(199708)65:43.O.CO;2-2).
- Gambacorti-Passerini C, et al. 2011. Multicenter independent assessment of outcomes in chronic myeloid leukemia patients treated with imatinib. *J Natl Cancer Inst* **103**:553–61. doi: [10.1093/jnci/djr060](https://doi.org/10.1093/jnci/djr060).
- Gerber DE, Minna JD. 2010. ALK inhibition for non-small cell lung cancer: from discovery to therapy in record time. *Cancer Cell* **18**:548–51. doi: [10.1016/j.ccr.2010.11.033](https://doi.org/10.1016/j.ccr.2010.11.033).
- Gillespie DT. 1977. Exact stochastic simulation of coupled chemical reactions. *J Phys Chem* **81**:2340–61. doi: [10.1021/j100540a008](https://doi.org/10.1021/j100540a008).
- Goldie JH, Coldman AJ. 1998. *Drug resistance in cancer: mechanisms and models*. New York: Cambridge University Press.
- Gonzalez-Angulo AM, Hortobagyi GN, Ellis LM. 2011. Targeted therapies: peaking beneath the surface of recent bevacizumab trials. *Nat Rev Clin Oncol* **8**:319–20. doi: [10.1038/nrclinonc.2011.66](https://doi.org/10.1038/nrclinonc.2011.66).
- Grupp SA, et al. 2013. Chimeric antigen receptor-modified T cells for acute lymphoid leukemia. *N Engl J Med* **368**:1509–18. doi: [10.1056/NEJMoa1215134](https://doi.org/10.1056/NEJMoa1215134).
- Gupta PB, Chaffer CL, Weinberg RA. 2009. Cancer stem cells: mirage or reality? *Nat Med* **15**:1010–2. doi: [10.1038/nm0909-1010](https://doi.org/10.1038/nm0909-1010).
- Haeno H, Iwasa Y, Michor F. 2007. The evolution of two mutations during clonal expansion. *Genetics* **177**:2209–21. doi: [10.1534/genetics.107.078915](https://doi.org/10.1534/genetics.107.078915).
- Hensel JA, Flaig TW, Theodorescu D. 2012. Clinical opportunities and challenges in targeting tumour dormancy. *Nat Rev Clin Oncol* **10**:41–51. doi: [10.1038/nrclinonc.2012.207](https://doi.org/10.1038/nrclinonc.2012.207).

- Hodi FS**, et al. 2010. Improved survival with ipilimumab in patients with metastatic melanoma. *N Engl J Med* **363**:711–23. doi: [10.1056/NEJMoa1003466](https://doi.org/10.1056/NEJMoa1003466).
- Katouli AA**, Komarova NL. 2010. Optimizing combination therapies with existing and future CML drugs. *PLOS ONE* **5**:e12300. doi: [10.1371/journal.pone.0012300](https://doi.org/10.1371/journal.pone.0012300).
- Katouli AA**, Komarova NL. 2011. The worst drug rule revisited: mathematical modeling of cyclic cancer treatments. *Bull Math Biol* **73**:549–84. doi: [10.1007/s11538-010-9539-y](https://doi.org/10.1007/s11538-010-9539-y).
- Khorashad JS**, et al. 2013. BCR-ABL1 compound mutations in tyrosine kinase inhibitor-resistant CML: frequency and clonal relationships. *Blood* **121**:489–98. doi: [10.1182/blood-2012-05-431379](https://doi.org/10.1182/blood-2012-05-431379).
- Kirkwood JM**, et al. 2012. Immunotherapy of cancer in 2012. *CA Cancer J Clin* **62**:309–35. doi: [10.3322/caac.20132](https://doi.org/10.3322/caac.20132).
- Komarova NL**, Wodarz D. 2005. Drug resistance in cancer: principles of emergence and prevention. *Proc Natl Acad Sci USA* **102**:9714–9. doi: [10.1073/pnas.0501870102](https://doi.org/10.1073/pnas.0501870102).
- Komarova NL**, Katouli AA, Wodarz D. 2009. Combination of two but not three current targeted drugs can improve therapy of chronic myeloid leukemia. *PLOS ONE* **4**:e4423. doi: [10.1371/journal.pone.0004423](https://doi.org/10.1371/journal.pone.0004423).
- Kwak EL**, et al. 2010. Anaplastic lymphoma kinase inhibition in non-small-cell lung cancer. *N Engl J Med* **363**:1693–703. doi: [10.1056/NEJMoa1006448](https://doi.org/10.1056/NEJMoa1006448).
- Lavi O**, Gottesman MM, Levy D. 2012. The dynamics of drug resistance: a mathematical perspective. *Drug Resist Updat* **15**:90–7. doi: [10.1016/j.drug.2012.01.003](https://doi.org/10.1016/j.drug.2012.01.003).
- Lenaerts T**, Pacheco JM, Traulsen A, Dingli D. 2010. Tyrosine kinase inhibitor therapy can cure chronic myeloid leukemia without hitting leukemic stem cells. *Haematologica* **95**:900–7. doi: [10.3324/haematol.2009.015271](https://doi.org/10.3324/haematol.2009.015271).
- Michor F**, et al. 2005. Dynamics of chronic myeloid leukaemia. *Nature* **435**:1267–70. doi: [10.1038/nature03669](https://doi.org/10.1038/nature03669).
- Michor F**, Nowak MA, Iwasa Y. 2006. Evolution of resistance to cancer therapy. *Current Pharm Des* **12**:261–71. doi: [10.2174/138161206775201956](https://doi.org/10.2174/138161206775201956).
- Misale S**, et al. 2012. Emergence of KRAS mutations and acquired resistance to anti-EGFR therapy in colorectal cancer. *Nature* **486**:532–6. doi: [10.1038/nature11156](https://doi.org/10.1038/nature11156).
- Porter K**, et al. 2003. Determinants of survival following HIV-1 seroconversion after the introduction of HAART. *Lancet* **362**:1267–74. doi: [10.1016/S0140-6736\(03\)14570-9](https://doi.org/10.1016/S0140-6736(03)14570-9).
- Reiter JG**, Bozic I, Chatterjee K, Nowak MA. 2013. TTP: Tool for Tumor Progression. In: *Proceedings of 25th International Conference on Computer Aided Verification, LNCS 8044*:101–6.
- Rew DA**, Wilson GD. 2000. Cell production rates in human tissues and tumours and their significance. Part II: clinical data. *Eur J Surg Oncol* **26**:405–17. doi: [10.1053/ejso.1999.0907](https://doi.org/10.1053/ejso.1999.0907).
- Sawyers C**. 2004. Targeted cancer therapy. *Nature* **432**:294–7. doi: [10.1038/nature03095](https://doi.org/10.1038/nature03095).
- Sequist LV**, et al. 2008. First-line gefitinib in patients with advanced non-small-cell lung cancer harboring somatic EGFR mutations. *J Clin Oncol* **26**:2442–9. doi: [10.1200/JCO.2007.14.8494](https://doi.org/10.1200/JCO.2007.14.8494).
- Shackleton M**, Quintana E, Fearon ER, Morrison SJ. 2009. Heterogeneity in cancer: cancer stem cells versus clonal evolution. *Cell* **138**:822–9. doi: [10.1016/j.cell.2009.08.017](https://doi.org/10.1016/j.cell.2009.08.017).
- Straussman R**, et al. 2012. Tumour micro-environment elicits innate resistance to RAF inhibitors through HGF secretion. *Nature* **487**:500–4. doi: [10.1038/nature11183](https://doi.org/10.1038/nature11183).
- Tomasetti C**, Levy D. 2010. Role of symmetric and asymmetric division of stem cells in developing drug resistance. *Proc Natl Acad Sci USA* **107**:16766–71. doi: [10.1073/pnas.1007726107](https://doi.org/10.1073/pnas.1007726107).
- Topalian SL**, et al. 2012. Safety, activity, and immune correlates of anti-PD-1 antibody in cancer. *N Engl J Med* **366**:2443–54. doi: [10.1056/NEJMoa1200690](https://doi.org/10.1056/NEJMoa1200690).
- Wilson TR**, et al. 2012. Widespread potential for growth-factor-driven resistance to anticancer kinase inhibitors. *Nature* **487**:505–9. doi: [10.1038/nature11249](https://doi.org/10.1038/nature11249).

Evolutionary dynamics of cancer in response to targeted combination therapy

Supplementary File 1: Mathematical Proofs

Bozic et al.

1 Notation

1.1 Resistance profiles

Consider a cancer therapy consisting of D targeted drugs, indexed $i = 1, \dots, D$. The resistance properties of each tumor cell can be summarized by its *resistance profile*, a binary string of length D , with 1's indicating which drugs the cell is resistant to. For example, the resistance profile 010 indicates that a cell is resistant to the second of three drugs, but sensitive to the first and third. The tumor is initiated by cells of type $0 \dots 0$ —sensitive to all drugs. Other profiles arise through resistance mutations. We let n_i denote the number of point mutations that would confer resistance to drug i . We also allow for the possibility that one point mutation may confer resistance to multiple drugs. The number of point mutations that would confer resistance to drugs i_1, \dots, i_m (but not to the other $D - m$ drugs), with $1 \leq i_1 < \dots < i_m \leq D$, is denoted $n_{i_1 \dots i_m}$. We disregard the possibility of losing drug resistance through mutation. Also, while our notation reflects an assumption that drug resistance arises via single point mutations, our results can readily be applied to situations in which multiple mutations are required for resistance to a single drug.

1.2 Branching process model

As described in the main text, we model the evolution of resistance as a stochastic branching process, in which each resistance profile is identified as a distinct type. Prior to treatment, all cell types divide at rate b and die at rate d . Thus the tumor expands at rate $r = b - d$ prior to treatment. Treatment is initiated when the tumor has reached a detection size of M cells. During treatment, we suppose that cell types sensitive to at least

one drug (i.e. those with resistance profiles other than $1 \dots 1$) divide and die at rates b' and d' , respectively, with $r' = b' - d' < 0$. Fully resistant cells (those with profile $1 \dots 1$) continue to divide and die at rates b and d , respectively. (More generally, one could suppose that each resistance profile has distinct birth and death rates during treatment, but we do not consider such generality here.)

With each reproduction, one of the daughter cells acquires each potential point mutation with probability equal to the point mutation rate u . (Our model assumes that only one of the daughter cells can acquire mutations, which amounts to rescaling the mutation rate by a factor of two.) Thus, for each combination of drugs i_1, \dots, i_m , the probability that one of the $n_{i_1 \dots i_m}$ resistance mutations occurs in a daughter cell is $(1 - u)^{n_{i_1 \dots i_m}} \approx 1 - n_{i_1 \dots i_m} u$. (This approximation assumes that $un_{i_1 \dots i_m} \ll 1$ —that is, resistance mutations are rare—so that the possibility of multiple resistance mutations in a single reproduction event can be disregarded.)

1.3 Paths to full resistance

We are most interested in the emergence of simultaneous resistance to all D drugs, leading to treatment failure. Such multi-drug resistance may occur via multiple paths, where a *path* is a sequence of resistance mutations leading from $0 \dots 0$ (no resistance) to $1 \dots 1$ (resistance to all drugs). An example for three drugs is the path $000 \rightarrow 010 \rightarrow 111$ (resistance to drug 2 first, then 1 and 3 simultaneously). Each path involves some number m of mutations, $1 \leq m \leq D$. Along a path there are $m + 1$ resistance profiles, indexed $j = 0, \dots, m$. The initial resistance profile $0 \dots 0$ is indexed $j = 0$, while the final, $1 \dots 1$, is indexed $j = m$. The number of potential point mutations that would lead from profile $j - 1$ to profile j , along a particular path, is denoted ν_j . The number of potential point mutations that would lead from profile $j - 1$ to a profile not on the path in question is denoted η_j . In short, ν_j and η_j are the numbers of “on-path” and “off-path” mutations, respectively, from profile $j - 1$. So, for example, for the path $000 \rightarrow 010 \rightarrow 111$ we have

$$\begin{aligned}\nu_1 &= n_2 \\ \eta_1 &= n_1 + n_3 + n_{12} + n_{13} + n_{23} + n_{123} \\ \nu_2 &= n_{13} + n_{123} \\ \eta_2 &= n_1 + n_3 + n_{12} + n_{23}.\end{aligned}$$

Thus, with each division of a cell of profile $j - 1$, we have the following probabilities of events (assuming $(\nu_j + \eta_j)u \ll 1$, i.e. resistance mutations

are rare):

$$\begin{cases} 1 - (\nu_j + \eta_j)u & \text{two daughters of profile } j - 1 \\ \nu_j u & \text{one daughter of profile } j - 1 \text{ and one of profile } j \\ \eta_j u & \text{one daughter of profile } j - 1 \text{ and one off-path daughter.} \end{cases}$$

1.4 The rare-mutation, large-tumor-size limit

In human cancers, the point mutation rate is very small ($u \sim 10^{-9}$) and the number of cells in a detectable tumor is very large ($M \sim 10^9$). Therefore, we concentrate on results that are asymptotically exact under the following limits:

$$u \rightarrow 0, \quad M \rightarrow \infty, \quad Mu^k = \text{constant}. \quad (1)$$

Above, k will be 1 or 2, depending on the result being presented. We will represent such a limit by the arrow $\xrightarrow[Mu^k = \text{const.}]{M \rightarrow \infty}$.

2 Number of resistant mutants at detection

We are first interested in following question: how many cells in the tumor are resistant to all D drugs at the time of detection?

2.1 Pathwise analysis

We begin by examining a single path, starting with fully sensitive cells (profile $0 \dots 0$, indexed $j = 0$), and ending with fully resistant cells (profile $1 \dots 1$, indexed $j = m$). For each $j = 0, \dots, m$, we let $x_j(t)$ denote the expected number of cells of profile j at time t . These expected numbers satisfy the following system of differential equations:

$$\dot{x}_j = (r - b(\nu_{j+1} + \eta_{j+1})u)x_j + b\nu_j u x_{j-1}. \quad (2)$$

Above, we set $x_{-1}(t) = 0$ for all t and $\nu_0 = \eta_0 = \nu_{m+1} = \eta_{m+1} = 0$. The initial conditions are $x_0(0) = 1$, and $x_j(0) = 0$ for $j = 1, \dots, m$.

We assume for the moment that $\nu_k + \eta_k \neq \nu_\ell + \eta_\ell$ for all pairs $k, \ell = 1, \dots, m$ with $k \neq \ell$. Under this assumption, the solution to the system (2)

is given by

$$x_j(t) = \begin{cases} e^{(r-b(\nu_1+\eta_1)u)t} & j = 0 \\ e^{rt} \left(\prod_{k=1}^j \nu_k \right) \sum_{k=1}^{j+1} \frac{e^{-b(\nu_k+\eta_k)ut}}{\prod_{\substack{1 \leq \ell \leq j+1 \\ \ell \neq k}} (\nu_\ell + \eta_\ell - \nu_k - \eta_k)} & 1 \leq j \leq m-1 \\ e^{rt} \left(\prod_{k=1}^m \nu_k \right) \left(\frac{1}{\prod_{\ell=1}^m (\nu_\ell + \eta_\ell)} - \sum_{k=1}^m \frac{e^{-b(\nu_k+\eta_k)ut}}{(\nu_k + \eta_k) \prod_{\substack{1 \leq \ell \leq m \\ \ell \neq k}} (\nu_\ell + \eta_\ell - \nu_k - \eta_k)} \right) & j = m. \end{cases} \quad (3)$$

We note that the above expressions for $x_j(t)$ are expectations over all possible trajectories, including those in which the tumor becomes extinct. Since we are only interested in tumors that grow to detectable size, we divide these expressions by the tumor survival probability, which is r/b . This yields an exact expression for the expected number of cells of each type at time t , conditioned on the survival of the tumor.

However, we wish to know the expected number of resistant cells not at a fixed time from when the tumor was initiated, but at the moment the total number of cells reaches M . The time T for the tumor to reach M cells is a random quantity; however, we can approximate T by using the deterministic growth law $x(t) = b/r e^{rt}$ for the total population of cells. (In other words, we set the total cell population equal to its expected value conditioned on non-extinction.) We then solve $x(T) = M$, yielding the approximation

$$T \approx \frac{1}{r} \log(Mr/b). \quad (4)$$

Simulation results (not shown) suggest that this approximation is exact in the large tumor size, small mutation rate limit (1).

We approximate the expected number x_m^{det} of fully resistant cells at detection (arising via this particular path) by substituting approximation (4)

for T into the expression for $x_m(t)$ given in (3). This yields

$$x_m^{\det} = M \left(\prod_{k=1}^m \nu_k \right) \left(\frac{1}{\prod_{\ell=1}^m (\nu_\ell + \eta_\ell)} - \sum_{k=1}^m \frac{e^{-\frac{b}{r}(\nu_k + \eta_k)u \log(Mr/b)}}{(\nu_k + \eta_k) \prod_{\substack{1 \leq \ell \leq m \\ \ell \neq k}} (\nu_\ell + \eta_\ell - \nu_k - \eta_k)} \right). \quad (5)$$

To simplify the above expression, we define $\mu = (b/r) u \log(Mr/b)$. We note that $\mu \rightarrow 0$ in the rare mutation, large tumor size limit $u \rightarrow 0$, $M \rightarrow \infty$, $Mu = \text{constant}$. Substituting μ into (5) and replacing $e^{-(\nu_k + \eta_k)\mu}$ by its Taylor expansion, we obtain

$$\begin{aligned} x_m^{\det} &= M \left(\prod_{k=1}^m \nu_k \right) \left(\frac{1}{\prod_{\ell=1}^m (\nu_\ell + \eta_\ell)} - \sum_{k=1}^m \frac{\sum_{s=0}^{\infty} \frac{\mu^s}{s!} (-\nu_k - \eta_k)^s}{(\nu_k + \eta_k) \prod_{\substack{1 \leq \ell \leq m \\ \ell \neq k}} (\nu_\ell + \eta_\ell - \nu_k - \eta_k)} \right) \\ &= M \left(\prod_{k=1}^m \nu_k \right) \left(\frac{1}{\prod_{\ell=1}^m (\nu_\ell + \eta_\ell)} - \sum_{s=0}^{\infty} \frac{\mu^s}{s!} \sum_{k=1}^m \frac{(-\nu_k - \eta_k)^s}{(\nu_k + \eta_k) \prod_{\substack{1 \leq \ell \leq m \\ \ell \neq k}} (\nu_\ell + \eta_\ell - \nu_k - \eta_k)} \right). \end{aligned} \quad (6)$$

For any collection of m distinct nonzero real numbers $\alpha_1, \dots, \alpha_m$ —in our case, we are interested in $\alpha_j = \nu_j + \eta_j$ —the following combinatorial identity holds:

$$\sum_{j=1}^m \frac{(-\alpha_j)^s}{\alpha_j \prod_{\substack{1 \leq \ell \leq m \\ \ell \neq j}} (\alpha_\ell - \alpha_j)} = \begin{cases} \frac{1}{\prod_{j=1}^m \alpha_j} & s = 0 \\ 0 & 1 \leq s \leq m-1 \\ -1 & s = m. \end{cases} \quad (7)$$

We save the proof of this identity for Section 7. Using this identity to simplify (6), we obtain

$$x_m^{\det} = M \left(\prod_{j=1}^m \nu_j \right) \frac{\mu^m}{m!} + \mathcal{O}(\mu^{m+1}). \quad (8)$$

Interestingly, this formula does not involve the numbers η_j of off-path mutations. As a consequence, we see that this result does not depend on the assumption that $\nu_k + \eta_k \neq \nu_\ell + \eta_\ell$ for $k \neq \ell$, and holds regardless of whether this condition is satisfied.

2.2 One drug

For single-drug therapy ($D = 1$), there is only one path to resistance, and the expected number of resistant cells at detection is given by (5), which simplifies to

$$x_{\text{res}}^{\text{det}} = M(1 - e^{-n_1\mu}) = Mn_1\mu + \mathcal{O}(\mu^2). \quad (9)$$

(We recall from above that $\mu = (b/r)u \log(Mr/b)$.)

2.3 Two drugs

For two-drug therapy, there are three paths to consider:

Path 1: $00 \rightarrow 10 \rightarrow 11$ In this case we have $\nu_1 = n_1$ and $\nu_2 = n_2 + n_{12}$. Using (8) we obtain

$$x_{\text{res},00 \rightarrow 10 \rightarrow 11}^{\text{det}} \approx Mn_1(n_2 + n_{12})\frac{\mu^2}{2} + \mathcal{O}(\mu^3).$$

Path 2: $00 \rightarrow 01 \rightarrow 11$ Similarly to path 1, we obtain

$$x_{\text{res},00 \rightarrow 01 \rightarrow 11}^{\text{det}} \approx Mn_2(n_1 + n_{12})\frac{\mu^2}{2} + \mathcal{O}(\mu^3).$$

Path 3: $00 \rightarrow 11$ Here $\nu_1 = n_{12}$. Using the exact solution (5) we obtain

$$x_{\text{res},00 \rightarrow 11}^{\text{det}} = M(1 - e^{-n_{12}\mu}) \approx M \left(n_{12}\mu - n_{12}^2 \frac{\mu^2}{2} \right) + \mathcal{O}(\mu^3).$$

Above, we have taken a second-order Taylor expansion of $e^{-n_{12}\mu}$.

Aggregating the above results, we obtain the following expression for the total expected number of resistant cells at detection:

$$x_{\text{res}}^{\text{det}} = M \left\{ n_{12}\mu + [2n_1n_2 + n_{12}(n_1 + n_2 - n_{12})] \frac{\mu^2}{2} \right\} + \mathcal{O}(\mu^3). \quad (10)$$

2.4 Arbitrary number of drugs with no cross-resistance

Suppose a therapy consists of $D \geq 1$ drugs, and there are no mutations that simultaneously confer resistance to multiple drugs. In this case, using (8), we obtain a remarkably simple formula for the expected number of resistant cells at detection:

$$x_{\text{res}}^{\text{det}} = Mn_1 \cdots n_D \mu^D + \mathcal{O}(\mu^{D+1}). \quad (11)$$

For example, in the case of triple therapy with no cross-resistance, we expect approximately $Mn_1n_2n_3\mu^3$ resistant cells at detection (accurate to order μ^4). Notice that the factorial in (8) is cancelled by the number, $D!$, of possible paths to full resistance.

3 Generating functions for branching processes

Generating functions are a powerful tool for analyzing stochastic processes. In a generating function, the probabilities of different events are recorded as coefficients in a power series, allowing these probabilities to be easily manipulated. Here we introduce the generating functions for the one- and two-type branching processes, which we will later use to derive probabilities of resistance and of treatment success.

3.1 One-type branching process

We first consider the one-type branching process. We introduce the random variable $Y(t)$ to represent the number of cells at time t , given that there was one such cell at time $t = 0$. The generating function for this process is then defined as

$$\phi_{m=1}(z; t) \equiv \mathbb{E} \left[z^{Y(t)} \right] \equiv \sum_{y=0}^{\infty} \mathbb{P}[Y(t) = y] z^y.$$

In words, the generating function is a time-dependent power series in which the coefficient of z^y equals the probability that there were y cells at time t . There is a well-known closed-form expression for this generating function (Athreya and Ney, 2004):

$$\phi_{m=1}(z; t) = \frac{d(1-z) + (zb-d)e^{-rt}}{b(1-z) + (zb-d)e^{-rt}}.$$

In particular, the probability that a lineage of type 1 cells survives for time t is given by

$$1 - \phi_{m=1}(0; t) = \frac{r}{b - de^{-rt}}. \quad (12)$$

3.2 Two-type branching process

We now turn to a branching process involving two types, labeled 1 and 2, with one-way mutation of rate $u\nu_2$ from type 1 to type 2. This process can be described by the following rates:

$$\begin{cases} 1 \rightarrow 11 & \text{rate } b \\ 1 \rightarrow \emptyset & \text{rate } d \\ 1 \rightarrow 12 & \text{rate } bu\nu_2 \\ 2 \rightarrow 22 & \text{rate } b \\ 2 \rightarrow \emptyset & \text{rate } d. \end{cases} \quad (13)$$

We introduce the random variables $Y_1(t)$ and $Y_2(t)$ to represent the numbers of type 1 and type 2 cells at time t , given that the process was initiated with a single type 1 cell at time $t = 0$. The generating function for this process is defined as

$$\phi_{m=2}(z_1, z_2; t) \equiv \mathbb{E} \left[z_1^{Y_1(t)} z_2^{Y_2(t)} \right] \equiv \sum_{y_1, y_2 \geq 0} \mathbb{P} [Y_1(t) = y_1, Y_2(t) = y_2] z_1^{y_1} z_2^{y_2}.$$

In words, the generating function is a time-dependent power series in the variables z_1 and z_2 , with the coefficient of $z_1^{y_1} z_2^{y_2}$ equal to the probability that there are y_1 cells of type 1 and y_2 cells of type 2 at time t .

A closed-form expression for this branching process was discovered by Antal and Krapivsky (2011). To state this solution, we first define the following constants:

$$\alpha = \frac{1}{2} \left[-(1 - u\nu_2) + \sqrt{(1 - u\nu_2)^2 + 4u\nu_2 \frac{b}{r}} \right],$$

$$\beta = 1 + \sqrt{(1 - u\nu_2)^2 + 4u\nu_2 \frac{b}{r}}.$$

Next, we let F denote the hypergeometric function ${}_2F_1$, and we define the following functions of a real number x :

$$\begin{aligned} F_1(x) &= F(\alpha, 1 + \alpha, \beta; x), \\ F_2(x) &= F(1 + \alpha - \beta, 2 + \alpha - \beta, 2 - \beta; x), \\ F_3(x) &= \frac{\alpha(1 + \alpha)}{\beta} F(1 + \alpha, 2 + \alpha, 1 + \beta; x), \\ F_4(x) &= \frac{(1 + \alpha - \beta)(2 + \alpha - \beta)}{2 - \beta} F(2 + \alpha - \beta, 3 + \alpha - \beta, 3 - \beta; x). \end{aligned}$$

Third, we define the following quantities, which depend on the arguments z_1 , z_2 , and t , of the generating function $\phi_{m=2}(z_1, z_2; t)$:

$$\begin{aligned} y_0 &= 1 - \frac{r}{b(1 - z_2)}, \\ \kappa &= \frac{1}{y_0} \left[\frac{b}{r}(z_1 - 1) - \alpha \right], \\ y &= y_0 e^{-rt}, \\ C &= y_0^\beta \frac{\kappa F_1(y_0) - F_3(y_0)}{(1 - \beta - \kappa y_0) F_2(y_0) + y_0 F_4(y_0)}. \end{aligned}$$

Finally, we state Antal and Krapivsky's (2011) formula for the generating function of the two-type branching process in terms of the above quantities and functions:

$$\phi_{m=2}(z_1, z_2; t) = 1 + \frac{r}{b}\alpha + \frac{r}{b} \frac{y^\beta F_3(y) + C(1 - \beta)F_2(y) + CyF_4(y)}{y^{\beta-1}F_1(y) + CF_2(y)}. \quad (14)$$

4 Probability of resistance at time of detection

We now turn to the question of whether at least one resistant cell exists at the time the tumor reaches detectable size. Again we consider each path to resistance separately.

4.1 One-step paths

A number of works (Coldman and Goldie, 1983; Dewanji et al., 2005; Komarova and Wodarz, 2005; Iwasa et al., 2006) have investigated the probability that resistance exists at the start of treatment, in the case that this resistance can be achieved through a single mutation. Here we follow the approach of Dewanji et al. (2005), in which we suppose that type 0 (sensitive) cells grow deterministically, and that type 1 (resistant) cells arise as a Poisson process, with rate depending on the current number of type 0 cells. Specifically, we approximate the growth of type 0 cells (conditioned on non-extinction) by

$$x_0(t) = \frac{b}{r} e^{rt}. \quad (15)$$

Noting that type 0 cells divide at rate b , and each division produces a type 1 mutant with probability $\nu\nu_1$, we suppose that type 1 (resistant) cells arise as a Poisson process with rate $b\nu\nu_1 x_0(t)$ at time t . Each line of type 1 cells

thus created is described by a one-type branching process initiated at the time of mutation.

We let the random variable $X_1(t)$ denote the number of type 1 cells at time t . The probability that there are no resistant cells at the time of detection ($T = 1/r \log(Mr/b)$) is equal to the probability that none of the type 1 mutations that arise in the interval $[0, T]$ survive to time T . The probability that a single type 1 mutation arising at time $0 \leq s \leq T$ survives until time T is given by $1 - \phi_{m=1}(0; T - s)$. Recalling that these mutations arise at rate $bu\nu_1 x_0(s)$ for $0 \leq s \leq T$, we can write this probability as

$$P[X_1(T) = 0] = \exp \left\{ - \int_0^T bu\nu_1 x_0(s) [1 - \phi_{m=1}(0; T - s)] ds \right\}.$$

Substituting from (12) and simplifying, we arrive at

$$\begin{aligned} P[X_1(T) = 0] &= \exp \left\{ -Mu\nu_1 \frac{b}{d} \log \left[\frac{b}{r} \left(1 - \frac{d}{rM} \right) \right] \right\} \\ &\xrightarrow[Mu=\text{const.}]{M \rightarrow \infty} \exp \left[-Mu\nu_1 \frac{b}{d} \log \left(\frac{b}{r} \right) \right]. \end{aligned} \quad (16)$$

This result was also obtained by Iwasa et al. (2006).

4.2 Two-step paths

We can apply similar methods to two-step paths ($m = 2$). The probability that, time t after a type 1 cell arises, this cell's lineage includes at least one surviving type 2 cell, can be written as $1 - \phi_{m=2}(1, 0, t)$. Thus a type 1 mutation that arises at time s , $0 \leq s \leq T$, will give rise to at least one living type 2 cell at time T , with probability $1 - \phi_{m=2}(1, 0, T - s)$. Following the arguments in the $m = 1$ case, the probability of no type 2 cells at time T can be written as

$$P[X_2(T) = 0] = \exp \left\{ - \int_0^T bu\nu_1 x_0(s) [1 - \phi_{m=2}(1, 0; T - s)] ds \right\}. \quad (17)$$

4.3 Low-mutation expansion for two-step paths

For low mutation rates, we can expand (17) as follows. First, we work through the construction of $\phi_{m=2}(z_1, z_2; t)$, substituting $z_1 = 1$ and $z_2 = 0$,

and expanding all quantities and functions to low orders in u . This yields:

$$\begin{aligned}\alpha &= \frac{b}{r}u\nu_2 + \mathcal{O}(u^2), \\ \beta &= 2 + \left(2\frac{b}{r} - 1\right)u\nu_2 + \mathcal{O}(u^2), \\ y_0 &= 1 - \frac{r}{b}, \\ \kappa &= -\frac{\alpha}{y_0} = -u\nu_2 \frac{b^2}{r(b-r)} + \mathcal{O}(u^2),\end{aligned}$$

$$\begin{aligned}F_1(x) &= 1 + \mathcal{O}(u), \\ F_2(x) &= 1 - x \frac{b/r - 1}{2b/r - 1} + \mathcal{O}(u), \\ F_3(x) &= -\frac{b}{r}u\nu_2 \frac{1}{x} \left[1 + \frac{1}{x} \log(1-x)\right] + \mathcal{O}(u^2), \\ F_4(x) &= -\frac{b/r - 1}{2b/r - 1} + \mathcal{O}(u), \\ C &= u\nu_2 \frac{b}{r} \log\left(\frac{b}{r}\right) + \mathcal{O}(u^2), \\ y(t) &= \left(1 - \frac{r}{b}\right) e^{-rt}.\end{aligned}$$

Combining the above expansions yields the following expansion for $\phi_{m=2}(1, 0; t) - 1$:

$$\phi_{m=2}(1, 0; t) - 1 = -u\nu_2 \frac{\log\left[\frac{b}{r} - \left(\frac{b}{r} - 1\right) e^{-rt}\right]}{\left(1 - \frac{r}{b}\right) e^{-rt}} + \mathcal{O}(u^2). \quad (18)$$

Substituting (18) into formula (17) for the probability of no resistance yields

$$\begin{aligned}\mathbb{P}[X_2(T) = 0] \\ = \exp\left\{-Mu^2\nu_1\nu_2 \frac{b^2}{b-r} \int_0^T \log\left[\frac{b}{r} - \left(\frac{b}{r} - 1\right) e^{-r(T-s)}\right] ds\right\} + \mathcal{O}(u^3)\end{aligned} \quad (19)$$

Above, we have also used the substitution $M = b/r e^{rT}$. We simplify the

integral in (19) as follows:

$$\begin{aligned}
& \int_0^T \log \left[\frac{b}{r} - \left(\frac{b}{r} - 1 \right) e^{-r(T-s)} \right] ds \\
&= \int_0^T \log \left[\frac{b}{r} - \left(\frac{b}{r} - 1 \right) e^{-rt} \right] dt \\
&= \log \left(\frac{b}{r} \right) T + \int_0^T \log \left[1 - \left(1 - \frac{r}{b} \right) e^{-rt} \right] dt.
\end{aligned}$$

The remaining integral above is positive and bounded above by

$$\int_0^\infty \log \left[1 - \left(1 - \frac{r}{b} \right) e^{-rt} \right] dt = \frac{1}{r} \text{Li}_2 \left(1 - \frac{r}{b} \right),$$

where Li_2 is the dilogarithm function. In particular, this bound is constant with respect to T , and therefore becomes negligible in comparison to $\log(b/r)T$ as T becomes large. This implies the following asymptotic formula for the integral in (19):

$$\int_0^T \log \left[\frac{b}{r} - \left(\frac{b}{r} - 1 \right) e^{-r(T-s)} \right] ds \xrightarrow{T \rightarrow \infty} \log \left(\frac{b}{r} \right) T.$$

Finally, substituting the above result into (19), and additionally substituting $T = \log(Mr/b)/r$, we obtain

$$\text{P} [X_2(T) = 0] \approx \exp \left[-Mu^2 \nu_1 \nu_2 \frac{b^2}{r(b-r)} \log \left(\frac{b}{r} \right) \log \left(\frac{Mr}{b} \right) \right]. \quad (20)$$

Our formulas (17) and (20) improve on results obtained by Haeno et al. (2007), as we discuss in Section 6.2.

4.4 Overall probability of resistance

One drug For a single drug, the probability that resistance exists at the time of detection can be obtained directly from (16) with $\nu_1 = n_1$, yielding

$$\begin{aligned}
p_{\text{res}} &= 1 - \exp \left\{ -Mun_1 \frac{b}{d} \log \left[\frac{b}{r} \left(1 - \frac{d}{rM} \right) \right] \right\} \\
&\xrightarrow[Mu=\text{const.}]{M \rightarrow \infty} 1 - \exp \left[-Mun_1 \frac{b}{d} \log \left(\frac{b}{r} \right) \right].
\end{aligned}$$

Two drugs For two drugs, we must consider the one-step path $00 \rightarrow 11$ and the two two-step paths $00 \rightarrow 10 \rightarrow 11$ and $00 \rightarrow 01 \rightarrow 11$. The probability that resistance exists at the time of detection equals one minus the probability that no cells of profile 11 are generated via any of these paths. We write this probability as $p_{\text{res}} = 1 - p_1 p_2$, where

$$p_1 = \exp \left[-M u n_{12} \frac{b}{d} \log \left(\frac{b}{r} \right) \right]$$

is obtained from (16) with $\nu_1 = n_{12}$, and

$$p_2 \approx \exp \left[-M u^2 (2n_1 n_2 + n_{12}(n_1 + n_2)) \frac{b^2}{r(b-r)} \log \left(\frac{b}{r} \right) \log \left(\frac{Mr}{b} \right) \right]$$

is obtained from (20) with $\nu_1 = n_1$, $\nu_2 = n_2 + n_{12}$ for the path $00 \rightarrow 10 \rightarrow 11$, and $\nu_1 = n_2$, $\nu_2 = n_1 + n_{12}$ for the path $00 \rightarrow 01 \rightarrow 11$. Rewriting in terms of $s = 1 - d/b$ yields the formulas for p_1 and p_2 presented in the main text.

5 Probability of tumor eradication

We now turn to the ultimate success or failure of multi-drug therapy. We define the therapy as successful if the tumor ultimately becomes extinct; otherwise, the tumor grows exponentially and there is a relapse. This differs from the question of analyzed in Section 4—the probability that resistance is present at the start of treatment—for two reasons. First, resistance that exists at the start of treatment may disappear due to stochastic drift. Second, new resistance mutations may appear during therapy.

We recall that, for all cell types sensitive to at least one drug (that is, all cells with resistance profiles other than $11 \dots 1$), the birth and death rates during treatment are denoted b' and d' , respectively, with $r' = b' - d' < 0$. Cells with resistance to all drugs are unaffected.

We separate the question of ultimate treatment outcome into resistance arising during tumor expansion and resistance arising during treatment. We let p^\uparrow and p^\downarrow denote the probability that no resistance mutations leading to relapse arise during expansion and treatment, respectively. The overall probability of eradication can then be written

$$p_{\text{erad}} = p^\uparrow p^\downarrow.$$

5.1 Resistance arising during expansion

We further separate into paths leading toward resistance.

5.1.1 One-step paths

As in Section 4.1, we suppose that type 1 (resistant) cells arise as a Poisson process with rate $b\nu_1 x_0(t)$ at time t , with $x_0(t) = b/r e^{rt}$. We also recall that each type 1 (resistant) mutation that arises has probability r/b of ultimately escaping stochastic drift (leading to unchecked tumor growth and patient relapse). Using similar reasoning to Section 4.1, the probability that no resistance mutations leading to treatment failure arise by this path, during tumor expansion, can be written as

$$\begin{aligned} p_{m=1}^\uparrow &= \exp \left[- \int_0^T b\nu_1 x_0(s) \frac{r}{b} ds \right] \\ &= \exp \left[-b\nu_1 \int_0^T e^{rs} ds \right] \\ &= \exp [-u\nu_1(M - b/r)] \\ &\xrightarrow[Mu=\text{const.}]{M \rightarrow \infty} e^{-Mu\nu_1}. \end{aligned} \tag{21}$$

This result was previously obtained by Komarova (2006, Appendix A).

5.1.2 Two-step paths

During the treatment phase, the lineage of each type 2 (fully resistant) cell will ultimately disappear with probability $\chi_2 = d/b$. For a type 1 cell that is present at the start of treatment, the probability χ_1 that its lineage will ultimately disappear can be obtained from the results of Antal and Krapivsky (2011):

$$\begin{aligned} \chi_1 &= \frac{1}{2} \left(1 + \frac{d'}{b'} + u\nu_2 \frac{r}{b} - \sqrt{\left(1 + \frac{d'}{b'} + u\nu_2 \frac{r}{b} \right)^2 - 4 \frac{d'}{b'}} \right) \\ &= 1 + u\nu_2 \frac{r}{b} \frac{b'}{r'} + \mathcal{O}(u^2). \end{aligned} \tag{22}$$

Above, b' and d' are the birth and death rates, respectively, of type 1 cells during treatment, and $r' = b' - d'$.

Suppose a type 1 mutation gives rise to y_1 type 1 cells and y_2 type 2 cells at the time of detection. Then the probability that all lineages of these cells disappear during treatment (and thus none of them cause eventual relapse) is $\chi_1^{y_1} \chi_2^{y_2}$. Overall, for a type 1 mutation that arises at time s , $0 \leq s \leq T$,

the probability that the lineage of this cell eventually disappears can be written as

$$\sum_{y_1, y_2 \geq 0} \mathbb{P} [Y_1(T-s) = y_1, Y_2(T-s) = y_2] \chi_1^{y_1} \chi_2^{y_2} = \phi_{m=2}(\chi_1, \chi_2, T-s).$$

Following the arguments of previous sections, the probability that no type 1 mutation leading to treatment failure arises during expansion can be written as

$$p_{m=2}^\dagger = \exp \left\{ - \int_0^T b u \nu_1 x_0(s) [1 - \phi_{m=2}(\chi_1, \chi_2; T-s)] ds \right\}. \quad (23)$$

This formula involves the expression $\phi_{m=2}(\chi_1, \chi_2; T-s)$. This expression cannot be evaluated directly using formula (14) for $\phi_{m=2}$, obtained by Antal and Krapivsky (2011), because this formula is undefined (has a removable singularity) at $z_2 = \chi_2 = d/b$. We therefore derive an expression for $\phi_{m=2}(z_1, d/b; t)$ from first principles. To begin, we note that dynamics of the two-type branching process (13) satisfy the backward Kolmogorov equations, which can be written as:

$$\begin{aligned} \partial_t \phi &= b\phi^2 + d + b\nu_2 u \phi \tilde{\phi} - (b + d + b\nu_2 u) \phi \\ \partial_t \tilde{\phi} &= b\tilde{\phi}^2 + d - (b + d) \tilde{\phi}. \end{aligned} \quad (24)$$

Above, $\phi \equiv \phi_{m=2}(z_1, z_2; t)$ is the generating function for the two-type process starting with a cell of type 1, while $\tilde{\phi}(z_1, z_2; t)$ is the analogous generating function starting with a cell of type 2. From the second equation in (24), we can see that

$$\tilde{\phi}(z_1, d/b; t) = d/b,$$

for all z_1 and all $t > 0$. Thus, for the fixed value $z_2 = \chi_2 = d/b$, the backward Kolmogorov equations (24) reduce to

$$\partial_t \phi = b\phi^2 - (b + d + r\nu_2 u) \phi + d.$$

This is a Ricatti equation with constant coefficients, which can be solved using standard techniques. We find the solution

$$\phi_{m=2}(z_1, \chi_2; t) = 1 - \frac{\frac{\theta_+ e^{b\theta_+ t}}{1 - z_1 - \theta_+} - \frac{\theta_- e^{b\theta_- t}}{1 - z_1 - \theta_-}}{e^{b\theta_+ t} - e^{b\theta_- t}}. \quad (25)$$

Above,

$$\theta_\pm = \frac{1}{2} \left[\frac{r}{b} (1 - u\nu_2) \pm \sqrt{\left(\frac{r}{b} (1 - u\nu_2) \right)^2 + 4u\nu_2 \frac{r}{b}} \right]. \quad (26)$$

5.1.3 Low-mutation expansion for two-step paths

We now derive an expression for $p_{m=2}^\uparrow$, the probability that no resistance arises via the path in question during tumor expansion, that is asymptotically exact in the limit of small mutation rate u and large detection size M . We know $\chi_2 = d/b$, and from (22) we have

$$\chi_1 = 1 + u\nu_2 \frac{r}{b} \frac{b'}{r'} + \mathcal{O}(u^2).$$

The formula (26) for θ_\pm admits the following low-mutation expansions:

$$\theta_+ = \frac{r}{b} + \mathcal{O}(u), \quad \theta_- = -u\nu_2 + \mathcal{O}(u^2).$$

We substitute these expansions into (25) and note that, for values of t that contribute significantly to the integral in (23) (with t identified as $T - s$), the terms containing e^{rt} eclipse those that are constant in t . As $u \rightarrow 0$ and $e^{rt} \rightarrow \infty$, we have

$$1 - \phi(\chi_1, \chi_2, t) \rightarrow \frac{r}{b} \left(1 + \frac{1}{u\nu_2 a} e^{-rt} \right)^{-1}, \quad a = \frac{b}{r} - \frac{b'}{r'}. \quad (27)$$

To obtain $p_{m=2}^\uparrow$ we substitute (27) into (23), which yields

$$p_{m=2}^\uparrow \xrightarrow[Mu^2=\text{const.}]{M \rightarrow \infty} \exp \left(-bu\nu_1 \int_0^T \frac{1}{e^{-rs} + A} ds \right), \quad A = (au\nu_2 e^{rT})^{-1}. \quad (28)$$

The integral on the right-hand side above simplifies as follows:

$$\int_0^T \frac{1}{e^{-rs} + A} ds = \frac{1}{Ar} \log \frac{1 + Ae^{rT}}{1 + A} \xrightarrow{e^{rT} \rightarrow \infty} \frac{1}{Ar} \log \frac{Ae^{rT}}{1 + A}.$$

Finally, by expressing everything in terms of the tumor size at detection, $M = b/r e^{rT}$, we arrive at

$$p_{m=2}^\uparrow \xrightarrow[Mu^2=\text{const.}]{M \rightarrow \infty} \exp \left[Mu^2 \nu_1 \nu_2 a \log \left(\frac{b}{rM} + u\nu_2 a \right) \right], \quad a = \frac{b}{r} - \frac{b'}{r'}. \quad (29)$$

5.2 Resistance arising during treatment

5.2.1 One-step paths

For one-step paths, the probability that no resistance arises during treatment was obtained by Michor et al. (2006):

$$p_{m=1}^\downarrow = \exp \left(Mu\nu_1 \frac{r}{b} \frac{b'}{r'} \right). \quad (30)$$

5.2.2 Two-step paths

During treatment, type 1 mutations arise from type 0 cells at rate $b'uv_1x_0(t)$ per unit time. Each such type 1 mutation has probability $1 - \chi_1$ of avoiding disappearance due to drift and eventually causing relapse, where χ_1 is the extinction probability given by (22). Thus the probability that no type 1 mutations leading to relapse arise during treatment is given by

$$\begin{aligned} p_{m=2}^\downarrow &= \exp \left[-b'uv_1 \int_0^\infty M e^{r's} (1 - \chi_1) ds \right] \\ &= \exp \left[\frac{b'}{r'} uv_1 M (1 - \chi_1) \right] \\ &\xrightarrow[Mu^2 = \text{const.}]{M \rightarrow \infty} \exp \left[-Mu^2 \nu_1 \nu_2 \frac{r}{b} \left(\frac{b'}{r'} \right)^2 \right]. \end{aligned} \quad (31)$$

5.3 Overall probability of tumor eradication

One drug For single-drug therapy, the probability of eradication is obtained by combining (21) and (30):

$$p_{\text{erad}} = p_{0 \rightarrow 1}^\uparrow p_{0 \rightarrow 1}^\downarrow = \exp \left(-Mu n_1 \frac{r}{b} a \right), \quad a = \frac{b}{r} - \frac{b'}{r'}.$$

Two drugs The probability of eradication for two-drug combination therapy can be written as $p_{\text{erad}} = p_1^\uparrow p_1^\downarrow p_2^\uparrow p_2^\downarrow$, where the subscript 1 refers to the path $00 \rightarrow 11$ and the subscript 2 refers to the paths $00 \rightarrow 10 \rightarrow 11$ and $00 \rightarrow 01 \rightarrow 11$. From (21) and (30) respectively, with $\nu_1 = n_{12}$, we have

$$p_1^\uparrow = \exp(-Mu n_{12}),$$

and

$$p_1^\downarrow = \exp \left(-Mu n_{12} \frac{r}{b} \frac{b'}{r'} \right).$$

From (30), and (31) respectively, with $\nu_1 = n_1$, $\nu_2 = n_2 + n_{12}$ for the path $00 \rightarrow 10 \rightarrow 11$, and $\nu_1 = n_2$, $\nu_2 = n_1 + n_{12}$ for the path $00 \rightarrow 01 \rightarrow 11$, we have

$$\begin{aligned} p_2^\uparrow &= \exp \left\{ Mu^2 a \left[n_1 (n_2 + n_{12}) \log \left(\frac{b}{rM} + u(n_2 + n_{12})a \right) \right. \right. \\ &\quad \left. \left. + n_2 (n_1 + n_{12}) \log \left(\frac{b}{rM} + u(n_1 + n_{12})a \right) \right] \right\}, \end{aligned}$$

and

$$p_2^\downarrow = \exp \left[-Mu^2(2n_1n_2 + n_{12}(n_1 + n_2)) \frac{r}{b} \left(\frac{b'}{r'} \right)^2 \right],$$

with $a = b/r - b'/r'$ as above. Substituting $r/b = s$ and $r'/b' = s'$ yields the formulas presented in the main text. We can also combine the above expressions to obtain

$$\begin{aligned} p_{\text{erad}} = \exp \bigg\{ & -Mun_{12} \frac{r}{b} a \\ & + Mu^2 n_1(n_2 + n_{12}) \left[\frac{r}{b} \left(\frac{b'}{r'} \right)^2 + a \log \left(\frac{b}{rM} + u(n_2 + n_{12})a \right) \right] \\ & + Mu^2 n_2(n_1 + n_{12}) \left[\frac{r}{b} \left(\frac{b'}{r'} \right)^2 + a \log \left(\frac{b}{rM} + u(n_1 + n_{12})a \right) \right] \bigg\}. \quad (32) \end{aligned}$$

Formula (32) improves on prior results of Komarova (2006), as we discuss in Section 6.3.

6 Comparison to previous results

Aspects of the dynamics of combination cancer therapy and resistance have been investigated in a number of previous works—notably Komarova and Wodarz (2005), Komarova (2006), and Haeno et al. (2007). Our results improve on the results previously obtained in these works and provide a closer match to simulations. This improvement is due in part to our use of recent advances in the theory of branching processes (Antal and Krapivsky, 2011), which allow us to obtain results that are asymptotically exact in the rare-mutation, large-tumor-size limit.

6.1 Expected number of resistant cells at detection

The question of the expected number of resistant cells in a tumor of detectable size has also been investigated by Iwasa et al. (2006), in the case of one drug, and Haeno et al. (2007), in the case of two drugs (with no mutations conferring resistance to both simultaneously).

For one drug, in the case that resistant cells have the same division and death rates as sensitive cells in the absence of treatment, formula (10) of Iwasa et al. (2006) gives the following expression for the expected number

of resistant cells:

$$x_{\text{res}}^{\text{det}} \approx M \frac{b}{r} n_1 u \log(M). \quad (33)$$

Comparing to our result (9), we see that Iwasa et al.'s coincides with ours (to first order in u) except that $\log(Mr/b)$ in (9) is replaced by $\log(M)$ in (33). This discrepancy arises from the fact that Iwasa et al. assume the sensitive cell population grows deterministically as e^{rt} , and do not condition on survival of the tumor. We compare Iwasa et al.'s formula (33) and ours (9) to simulation results in Table S1.

In the case of two drugs, Haeno et al. (2007) derive the following expression for the average number resistant cells:

$$x_{\text{res}}^{\text{det}} \approx 2 \left(\frac{b}{r} \right)^2 n_1 n_2 u^2 \sum_{x=1}^{M-1} \frac{M}{x} \log \frac{M}{x}. \quad (34)$$

Upon applying the approximation

$$\sum_{x=1}^{M-1} \frac{M}{x} \log \frac{M}{x} \approx \int_1^M \frac{M}{x} \log \frac{M}{x} dx = \frac{1}{2} M \log(M)^2,$$

formula (34) becomes

$$x_{\text{res}}^{\text{det}} \approx \left(\frac{b}{r} \right)^2 n_1 n_2 u^2 \log(M)^2.$$

As in the result of Iwasa et al. (2006), this expression differs from ours only in the replacement of $\log(Mr/b)$ by $\log(M)$, which again arises because Haeno et al. do not condition on survival of the tumor. We compare this expression to our formula (10) in Table S2.

For three or more drugs (or for drug resistance requiring three or more mutational steps) our formulas (5), (8), and (11) provide the first closed-form expressions for the expected number of fully resistant cells at time of detection.

6.2 Probability of resistance at detection

Haeno et al. (2007) also derive expressions for $P[X_2(T) > 0]$, the probability that resistance requiring two mutational steps is present at the time of detection. Their expressions are derived using approximate solutions to the differential equations that define the generating function $\phi_{m=2}(z_1, z_2; t)$

M	n_1	Simulation	This work, Eq. (9)	Iwasa et al., Eq. (33)
10^5	1	53	50	58
10^5	10	510	494	575
10^5	100	4900	4831	5754
10^7	1	76	73	81
10^7	10	740	725	806
10^7	100	7400	7252	8059
10^9	1	96	96	104
10^9	10	920	956	1036
10^9	100	9800	9557	10361

Table S1: Comparison of formulas and simulation results for the expected number of resistant cells at detection for the case of one drug. Parameter values are $b = 0.25$, $d = 0.2$, and $u = 1/M$ for each value of M . 10^8 simulation runs were used per parameter combination.

M	n_1	n_2	Simulation	This work, Eq. (10)	Haeno et al., (34)
10^5	10	10	2.7	2.5	3.6
10^5	100	100	250	245	365
10^5	1000	1000	14000	24520*	36133
10^7	10	10	0.05	0.05	0.07
10^7	100	100	5.6	5.26	6.96
10^7	1000	1000	550	526	696
10^9	10	10	0.001	0.001	0.001
10^9	100	100	0.09	0.09	0.11
10^9	1000	1000	9.4	9.1	11.3

Table S2: Comparison of formulas and simulation results for the expected number of resistant cells at detection for the case of two drugs. Parameter values: $b = 0.25$, $d = 0.2$, $u = 1/M$, $n_{12} = 0$. 10^8 simulation runs were used per parameter combination. *The high degree of inaccuracy for this parameter combination occurs because $un_1 = un_2 = 10^{-2}$ is sufficiently large to introduce errors in approximations that assume $un_i \ll 1$.

M	Sim.	This work, Eq. (17) (exact)	This work, Eq. (20) (closed-form)	Haeno et al., Eq. (35)	Haeno et al., Eq. (36)
5×10^8	0.10	0.10	0.17	0.32	0.029
1×10^9	0.20	0.20	0.32	0.57	0.051
2×10^9	0.36	0.35	0.55	0.9	0.09
3×10^9	0.48	0.48	0.70	*	0.12
5×10^9	0.67	0.66	0.88	*	0.17
1×10^{10}	0.89	0.89	0.98	*	0.27

Table S3: Probability p_{res} of resistance at detection for dual therapy with no cross-resistance, as calculated using simulation, using our formulas (17) and (20), and using the formulas (35) and (36) of Haeno et al. (2007). Parameter values are $u = 10^{-8}$, $n_1 = n_2 = 100$, $b = b' = 0.25$, $d = 0.2$. *Here Haeno et. al's formula fails by giving a probability greater than 1.

(see Appendix A). In contrast, our formulas (17) and (20) for $P[X_2(T) = 0]$ utilize the exact solution obtained by Antal and Krapivsky (2011).

The two formulas derived by Haeno et al. (2007) both describe the probability that, at the time of detection, at least one cell contains two mutations arising in a specified order. (In other words, their formulas apply to the case of a particular two-step path.) Their main formula can be expressed in our notation as

$$P[X_2(T) > 0] = -\frac{Mu^2\nu_1\nu_2 \log(u\nu_2)}{(1 - d/b)^2}. \quad (35)$$

They also present an alternative formula:

$$P[X_2(T) > 0] = \sum_{x=1}^M e^{-u\nu_1(x-1)} (1 - e^{-u\nu_1}) \left[1 - \exp\left(-\frac{Mu_2}{(1 - d/b)(x+1)}\right) \right]. \quad (36)$$

In Table S3 we compare values of the overall probability of no resistance at detection p_{res} (along all paths) as obtained from simulation, as derived from our formulas (17) and (20), and as derived from formulas (35) and (36) of Haeno et al. (2007).

6.3 Probability of tumor eradication

Turning to the question of whether therapy will successfully eradicate a tumor, our results in the case of one-step paths to resistance agree with

those of Komarova (2006) and Michor et al. (2006), as noted where these results are presented.

For two-step paths, Komarova (2006) obtained closed-form approximations for the probability of tumor eradication, in the special case that an equal number of mutations are required for each step ($\nu_1 = \nu_2$), and that treatment affects only the death rate of tumor cells, not the division rate ($b' = b$).

Komarova’s (2006) expression for the probability p^\uparrow —that no mutations leading to eventual relapse arise during tumor expansion—can be expressed in our notation as

$$p^\uparrow = 1 - M(u\nu)^2 \frac{b}{r} \log \left(\frac{M}{M_0} - 1 \right). \quad (37)$$

Above, $\nu = \nu_1 = \nu_2$ is the number of resistance mutations at each step, and M_0 is an extra parameter representing tumor’s initial size. Our approach of considering the entire history of the tumor, conditioned on its survival, amounts to setting $M_0 = b/r$. (We also note that Komarova uses P^\uparrow and P^\downarrow to denote the probabilities that mutations leading to relapse *do* arise during the two respective phases; thus P^\uparrow in Komarova’s notation corresponds to $1 - p^\uparrow$ in ours, and similarly for P^\downarrow and p^\downarrow .)

The approximation (37) for p^\uparrow is based on first determining the probability that at least one type 2 mutation arises, then multiplying that quantity by the survival probability of each such mutation. This method is accurate if few type 2 mutants are likely to be generated ($Mu^2\nu^2 \lesssim 1$), but loses accuracy if many type 2 mutations may arise, because it does not take into account the individual fate of each mutation. Our expression (29), based on the exact formula for $\phi_{m=2}(z_1, z_2; t)$ obtained by Antal and Krapivsky (2011), does not have this limitation.

For the probability p^\downarrow that no mutations leading to relapse arising during treatment, Komarova (2006) obtained

$$p^\downarrow = \left[1 - (u\nu)^2 \frac{br}{(r')^2} \right]^M \approx \exp \left[-M(u\nu)^2 \frac{br}{(r')^2} \right]. \quad (38)$$

This expression coincides with our formula (31) in the special case $\nu_1 = \nu_2 = \nu$ and $b' = b$. Our result (31) can therefore be seen as a generalization of Komarova’s result (38) to the case that mutation numbers may be unequal and treatment may affect tumor cell division rates.

Table S4 compares our formula (32) for the overall probability p_{erad} of tumor eradication for two-drug therapy to the results of Komarova (2006).

M	Simulation	This work, Eq. (32)	Komarova (2006)
10^9	0.79	0.79	0.80
2×10^9	0.63	0.62	0.59
3×10^9	0.50	0.49	0.38
4×10^9	0.39	0.38	0.17
5×10^9	0.31	0.30	*

Table S4: Probability p_{erad} of tumor eradication as calculated using simulation, using our formula (32), and using the formulas (37) and (38) of Komarova (2006). Parameter values are $u = 10^{-8}$, $n_1 = n_2 = 100$, $b = b' = 0.25$, $d = 0.2$, $d' = 0.3$. *Here Komarova's formula fails by giving a negative answer.

Finally, we note that Komarova (2006) also provides computational recipes to obtain probabilities for treatment success to arbitrary numerical precision. This methodology has been applied to a number of specific questions regarding treatment of chronic myeloid leukemia (Komarova and Wodarz, 2005; Komarova et al., 2009; Katouli and Komarova, 2010; Komarova, 2011).

7 Proof of Identity (7)

In this section we prove the mathematical identity used in Section 2.1. We state this identity in an equivalent form:

Theorem 1. *For any collection of m distinct nonzero real numbers $\alpha_1, \dots, \alpha_m$ and any integer $0 \leq s \leq m$,*

$$\sum_{j=1}^m \frac{\alpha_j^{s-1}}{\prod_{\substack{1 \leq \ell \leq m \\ \ell \neq j}} (\alpha_\ell - \alpha_j)} = \begin{cases} \frac{1}{\prod_{\ell=1}^m \alpha_\ell} & s = 0 \\ 0 & 1 \leq s \leq m-1 \\ (-1)^{m+1} & s = m. \end{cases} \quad (39)$$

Proof. Our proof is based on Cauchy's residue theorem of complex analysis. Consider the meromorphic function

$$F(z) = \frac{z^{s-1}}{\prod_{\ell=1}^m (\alpha_\ell - z)}.$$

Now consider a closed curve γ in the complex plane, whose interior contains the points $\alpha_1, \dots, \alpha_m$, as well as zero. Applying the residue theorem and

Cauchy's integral formula yields

$$\frac{1}{2\pi i} \oint_{\gamma} F(z) dz = \begin{cases} -\sum_{j=1}^m \frac{\alpha_j^{s-1}}{\prod_{\substack{1 \leq \ell \leq m \\ \ell \neq j}} (\alpha_{\ell} - \alpha_j)} & s \geq 1 \\ -\sum_{j=1}^m \frac{\alpha_j^{s-1}}{\prod_{\substack{1 \leq \ell \leq m \\ \ell \neq j}} (\alpha_{\ell} - \alpha_j)} + \frac{1}{\prod_{\ell=1}^m \alpha_{\ell}} & s = 0. \end{cases} \quad (40)$$

On the other hand, since F has no poles outside of γ other than possibly at ∞ (in the case $s \geq m$) we can also express this integral in terms of the residue of F at ∞ :

$$\begin{aligned} \frac{1}{2\pi i} \oint_{\gamma} F(z) dz &= \text{Res}[F(z), \infty] \\ &= \text{Res}[z^{-2}F(z^{-1}), 0]. \end{aligned}$$

We rewrite

$$\begin{aligned} z^{-2}F(z^{-1}) &= \frac{z^{-s-1}}{\prod_{\ell=1}^m (\alpha_{\ell} - z^{-1})} \\ &= \frac{z^{m-s-1}}{\prod_{\ell=1}^m (\alpha_{\ell} z - 1)}. \end{aligned}$$

Cauchy's integral formula then gives

$$\text{Res}[F(z), \infty] = \begin{cases} 0 & 0 \leq s \leq m-1 \\ \frac{1}{(m-s)!} \left. \frac{d^{m-s}}{dz^{m-s}} \right|_{z=0} \frac{1}{\prod_{\ell=1}^m (\alpha_{\ell} z - 1)} & s \geq m. \end{cases}$$

In particular, for $s = m$ we have $\text{Res}[F(z), \infty] = (-1)^m$. Combining with (40) verifies the desired result (39), and moreover, provides a method to calculate similar expressions with $s > m$. \square

References

Antal, T. and P. L. Krapivsky (2011). Exact solution of a two-type branching process: models of tumor progression. *Journal of Statistical Mechanics: Theory and Experiment* 2011(08), P08018.

- Athreya, K. B. and P. E. Ney (2004). *Branching Processes*. Dover Publications.
- Coldman, A. J. and J. H. Goldie (1983). A model for the resistance of tumor cells to cancer chemotherapeutic agents. *Mathematical Biosciences* 65(2), 291–307.
- Dewanji, A., E. Luebeck, and S. Moolgavkar (2005). A generalized luria–delbrück model. *Mathematical Biosciences* 197(2), 140–152.
- Haeno, H., Y. Iwasa, and F. Michor (2007). The evolution of two mutations during clonal expansion. *Genetics* 177(4), 2209–2221.
- Iwasa, Y., M. A. Nowak, and F. Michor (2006). Evolution of resistance during clonal expansion. *Genetics* 172(4), 2557–2566.
- Katouli, A. A. and N. L. Komarova (2010). Optimizing combination therapies with existing and future cml drugs. *PloS one* 5(8), e12300.
- Komarova, N. (2006). Stochastic modeling of drug resistance in cancer. *Journal of Theoretical Biology* 239(3), 351–366.
- Komarova, N. L. (2011, Apr). Mathematical modeling of cyclic treatments of chronic myeloid leukemia. *Math Biosci Eng* 8(2), 289–306.
- Komarova, N. L., A. A. Katouli, and D. Wodarz (2009, 02). Combination of two but not three current targeted drugs can improve therapy of chronic myeloid leukemia. *PLoS ONE* 4(2), e4423.
- Komarova, N. L. and D. Wodarz (2005). Drug resistance in cancer: Principles of emergence and prevention. *Proceedings of the National Academy of Sciences of the United States of America* 102(27), 9714–9719.
- Michor, F., M. A. Nowak, and Y. Iwasa (2006). Evolution of resistance to cancer therapy. *Current Pharmaceutical Design* 12(3), 261–271.